Danish Climate Centre

DMI, Ministry of Transport

A time-slice experiment with the ECHAM4 A-GCM at high resolution: The simulation of tropical storms for the present-day and of their change for the future climate

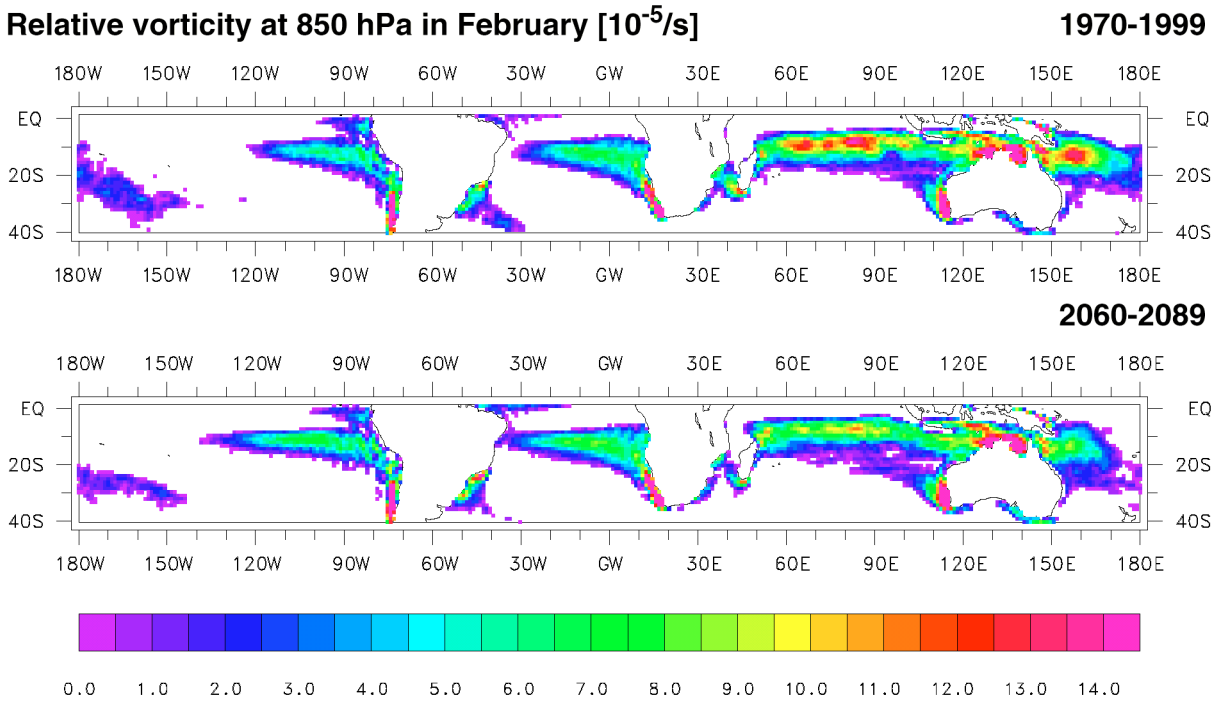

Wilhelm May

Danish Meteorological Institute
and Danish Climate Centre

Report 00-5

A time-slice experiment with the ECHAM4 A-GCM at high resolution:
The simulation of tropical storm for the present-day and the their change for the future climate

Danish Climate Centre, Report 00-5

Wilhelm May

ISSN: 1398-490-X
ISSN: 1399-1957 (Online)
ISBN: 87-7478-423-4

Danish Meteorological Institute
Lyngbyvej 100
DK-2100 Copenhagen Ø
Denmark

Phone: +45 3915 7500
Fax: +45 3927 1080
www.dmi.dk

Abstract

The ECHAM4 atmospheric GCM's capability to simulate tropical cyclones for the present-day climate is studied and the possible changes in their characteristics, i.e., their frequency and intensity for the future climate is assessed. This is done on the basis of an extended time-slice experiment using ECHAM4 at high resolution, i.e., T106 in triangular spectral truncation. The two time-slices cover a period of 30 years each representing both the present-day (1970-1999) and the future (warmer) climate (2060-2089).

The tropical storms simulated by ECHAM4 are unrealistically weak and, hence, occur much less frequently than in reality, i.e., at about 55% of the time. By this ECHAM4 differs substantially from the previous version of the ECHAM model (ECHAM3), which has been capable to simulate quite realistic tropical storms. This indicates the delicate balance between the different model components, at which GCMs are able to simulate tropical cyclones reasonably well. The time-slice experiment predicts a substantial reduction of the number of tropical storms in the future climate, i.e., about 25%. The reduction is somewhat larger in the Southern than in the Northern Hemisphere. Along with this reduction of the frequency goes a general reduction of the intensity of the tropical cyclones. These changes in the characteristics of tropical cyclones can be related to large-scale changes of the circulation in the tropics leading to less favourable dynamical conditions for the developments of storms, while the general warming of the sea surface temperatures in the tropics should favour more and/or more intense cyclones in the future.

1. Introduction

The possibility of climate change caused by the ongoing rapid increase of various greenhouse gases, with carbon dioxide (CO_2) being considered the most important one, has been intensively investigated over the last decade. Though the question that an overall warming of the earth's atmosphere will take place is widely accepted within the scientific community, there is still some disagreement regarding the magnitude of the change and the question, how long it may take, before the change becomes indisputably noticeable (Houghton et al., 1990; 1996). The major tool to assess the anticipated change in climate caused by the increase of greenhouse gases are simulations with global coupled atmosphere-ocean models, where the changes of the concentrations of various greenhouse gases have been prescribed according to typical scenarios provided by the Intergovernmental Panel on Climate Change (IPCC) (e.g., Mitchell et al., 1995). During the last decade the models used for these scenario simulations have gradually been refined, not only with respect to the physical parameterizations and the resolution but also with respect to the external forcing mechanisms. While earlier studies were based on models with relatively coarse resolutions of about 5° to 6° (e.g., Manabe et al., 1991; Cubasch et al., 1992), the horizontal resolution is roughly doubled in the current generation of models (e.g., Mitchell and Johns, 1997). Some models consider not only CO_2 but other greenhouse gases as well, such as methane (CH_4), nitrous oxide (N_2O), chlorofluorocarbons (CFCs) and other industrial gases, tropospheric ozone and also the direct and indirect effects of sulphate aerosols (e.g., Roeckner et al., 1999). In spite of these improvements the uncertainties in the assessment of future climate change are still quite large. These uncertainties are, for instance, related to a number of atmospheric feed-back processes, which are treated differently in the different models. Another source of uncertainty is the heat uptake by the ocean, which affects both the pattern and the delay of the warming induced by the radiative forcing of the greenhouse gases. Therefore, it would be desirable to assess the future climate change on the basis of an ensemble of simulations with a number of different climate models.

Even though an overall change in the mean climate, i.e., the mean temperature and the mean amount of precipitation will have some consequences for mankind, the possible changes in the extremes of weather and climate will have very strong social and economic impacts on the human society (e.g., Kunkel et al., 1999). Such extreme events include floods and droughts, intense heat and cold waves, but also intense cyclones both in the tropics and in the extratropics or thunderstorms. In the United States (US), for instance, the damages and fatalities due to

floods have increased over the last 25 years, which may in part be due to an increase in the frequency of heavy rain events (e.g., Kunkel et al., 1999). There has also been a steady increase in hurricane losses, which, however, can be related to changes in population, inflation and wealth. Winter storm damages, on the other hand, have increased over the last 10-15 years partially due to an increase in the frequency of intense storms in the northeast. Further, the IPCC stated in its report (Watson et al., 1996) that "reinsurers have noticed a fourfold increase in disasters since the 1960s. This is not due merely to better recording, because the major disasters - which account for 90% of the losses and would always be recorded - have increased just as quickly. Much of the rise is due to socioeconomic factors, but many insurers feel that the frequency of extreme events has also increased." Among these extreme weather events, tropical cyclones are by far the most devastating ones, with respect to fatalities as well as with respect to economic losses. More than 300,000 people were, for instance, killed by the tropical storm, which affected Bangladesh about 30 years ago, and the hurricane Andrew caused economic losses of about 30 billion US dollars in the US in 1992.

It is therefore of major interest to assess, whether the frequency as well as the intensity of tropical cyclones changes in a future climate, which is generally warmer due to the increase in the atmospheric concentrations of the important greenhouse gases. This is, however, a quite difficult task, since as stated in the IPCC report (Houghton et al., 1996) that "the state-of the-science [tropical cyclone simulations in greenhouse conditions] remain poor because (i) tropical cyclones cannot be adequately simulated in present GCMs [general circulation models]; (ii) some aspects of ENSO [El Niño/Southern Oscillation] are not well simulated in GCMs; (iii) other large-scale changes in the atmospheric general circulation which could affect tropical cyclones cannot yet be discounted; and (iv) natural variability of tropical storms is very large, so small trends are likely to be lost in the noise." It was thus concluded that "it is not possible to say whether the frequency, area of occurrence, mean intensity or maximum intensity of tropical cyclones will change." Since then (the IPCC assessment was undertaken in 1994 and early 1995) the research efforts focusing on the potential changes in tropical cyclone activity in a warmer climate has, however, proceeded, and a review of that work is given in Henderson-Sellers et al. (1998).

Several observational studies have indicated trends in the tropical storm activity in various regions, but should be taken with cautiousness, since these long-term variations are hampered by relatively short periods with accurate observations. Nicholls et al. (1998) observed,

for instance, a decline of the number of tropical cyclones in the Australian region since the season 1969/70. This trend was mainly accounted for by a decrease in the frequency of weak and moderate systems, while the number of more intense systems is slightly increased. The authors could, however, not rule out that this decline was primarily artificial due to changes in the tropical cyclone analysis procedures. Chan and Shi (1996) found that over the northwestern Pacific both the number of typhoons (surface winds reach 33 m/s (Neumann, 1993)) and the total number of tropical storms had increased since 1980. This increase had, however, been preceded by a nearly identical decrease between about 1960 and 1980. The inspection of the number of tropical storms over the Atlantic did not lead to any significant trend (Landsea et al. 1996), but the number of hurricanes (surface winds reach 33 m/s (Neumann, 1993)) exhibited a pronounced downward trend from the 1940s through the 1990s. In addition to these changes in frequency, there has been a reduction in the mean intensity of Atlantic tropical storms but no significant change in the maximum intensity reached by the strongest hurricane each year.

The problem of predicting possible changes of the frequency and the intensity of tropical storms in a warmer climate can be separated in two parts: a) the prediction of how the atmosphere's and the ocean's capability to sustain tropical cyclones may change and b) the prediction of how the frequency and strength of initiating disturbances may change. Over the last 10 years several studies have used GCMs in order to address this issue and tried to infer changes in the tropical cyclone activity by analysing the vortices at the resolvable scale of these models. These studies have, however, lead to conflicting results. Broccoli and Manabe (1990) performed a set of experiments with the Geophysical Fluid Dynamics Laboratory (GFDL) GCM at different horizontal resolutions and with a different treatment of clouds. In one set the cloudiness was prescribed and in the other set the cloud amount was variable. In the experiments with prescribed clouds the authors inferred an increase in both the number and duration of tropical cyclones in a doubled CO_2 climate, but a significant reduction in the experiments with variable clouds. This finding did, however, not depend on the horizontal resolution of the model, that were R15 (4.5° lat. × 7.5° lon.) and R30 (2.25° lat. × 3.75° lon.). In a similar study based on a version of the United Kingdom Meteorological Office (UKMO) GCM Haarsma et al. (1993) found an increase in the frequency of simulated tropical storms by about 50% in the doubled CO_2 conditions. The model's resolution was R30, and the cloud amount was variable. Bengtsson et al. (1996) (referred to as "B96" in the following), who used a high-resolution GCM (T106, corresponding to 1.125° lat. × 1.125° lon.), obtained a substantial reduction of

the number of tropical storms in a warmer climate, in particular in the Southern Hemisphere, while the geographical distribution of the simulated tropical cyclones did not change as compared to their simulation of the present-day climate. Different to the preceding studies employing low-resolution models (e.g., Broccoli and Manabe, 1990; Haarsma et al., 1993), Bengtsson et al. (1995) (referred to as "B95" in the following) identified much more realistic structures and intensities of the tropical cyclones in their simulations at high resolution.

In a study with a limited-area model Walsh and Watterson (1997) identified two main limitations of climate models that constrain the models' capability of simulating relatively small and convective-driven systems such as tropical cyclones. That are the coarse horizontal and vertical resolutions as well as inadequate representations of moist convective processes in these models. In a recent study Knutson et al. (1998) and Knutson and Tuleya (1999) used, in fact, a regional high-resolution hurricane prediction model in order to investigate the impact of climate warming on the intensity of tropical storms over the northwestern Pacific. They found that for an average warming of the sea surface temperatures (SSTs) by about 2.2° C the simulations yielded typhoons that were more intense by 3 to 7 m/s for the wind speed and 7 to 20 hPa for the central surface pressure in a warmer climate. In their study the authors have rerun about 50 cases from a control and from a high CO_2 simulation for a 5-day period each with the high-resolution GFDL Hurricane Prediction System (Kurihara et al., 1998). The simulated tropical storms were quite realistic except for a slight underprediction of the wind speeds in the strongest storms in the control cases.

Encouraged by the results of B95 and B96 we want to assess the possible changes of the frequency and the intensity of tropical storms in a warmer climate in this study. This is done on the basis of an extended time-slice experiment with the ECHAM4 atmospheric GCM at high resolution (May, 1999; May and Roeckner, 2000). Our experiment differs, however, from a similar experiment with the ECHAM3 model used in B96 in two aspects. Firstly, our experiment extends over two periods of 30 years for the simulation of the present-day and the future climate, whereas B96 could analyse only 5 years of data for each simulation. By that we have reduced the effects of the relatively large internal variability (e.g., Henderson-Sellers et al., 1998), which, as pointed out in B96, may affect the stability of the results. Secondly, we have chosen a somewhat different experimental approach for our time-slice experiment than in B96 allowing for interannual variations of the SSTs. By that we have been able to incorporate such a prominent phenomenon as ENSO, which has been found to have an influence on the tropical

storm activity in different basins. In the Australian region, for instance, the higher than normal pressure over Australia associated with El Niño events leads to a reduced number of tropical cyclones (Nicholls, 1984; Evans and Allen, 1992), while the centre of tropical cyclone activity moves toward the equator and the frequency of cyclone development increases east of 170° W (Revell and Goulter, 1986; Evans and Allen, 1992). During La Niña events these trends are reversed. Consistent with these findings, over the northwestern Pacific reduced numbers of tropical cyclone genesis have been found west of 160° E, but increased cyclogenesis in a region east of 160° E and south of 20° N during El Niño events (Chan, 1985; Lander, 1994). The opposite behaviour has been identified during La Niña events. Jones and Thorncroft (1998) observed, on the other hand, a relatively low number of tropical cyclones over the Atlantic during both the strong El Niño events in 1983 and 1997.

Broccoli and Manabe (1990) raised the general question, whether GCMs were appropriate tools in order to examine the mechanisms coupling the greenhouse warming with the tropical cyclone activity. B96 answered this question affirmative, since their model (ECHAM3) had been capable to simulate the structures and intensities of tropical cyclones rather realistically. Nevertheless one should keep in mind the finding by Broccoli and Manabe (1990), according to which the sign of the change in the number and duration of tropical cyclones in a doubled CO_2 climate depended on the treatment of clouds in their model. Compared to the previous version of the ECHAM model (ECHAM3), the recent version (ECHAM4) has undergone major changes in both the numerical methods and the physical parameterizations (Roeckner et al., 1996a). This includes the parameterizations of cumulus convection and radiation, which may effect the development of tropical storms in the GCM. Hence, it is of interest to know, whether ECHAM4 is capable to simulate the structures and intensities of tropical cyclones as realistically as ECHAM3 and what changes of the frequency and the intensity of tropical storms in a warmer climate can be inferred from our time-slice experiment with ECHAM4.

The paper is organized as follows: In section 2 we describe the time-slice experiment, on which our study is based, and in section 3 the criteria, by which we have identified tropical storms. Subsequently the results for the present-day climate (section 4) and for the future climate (section 5) are presented. A discussion and some concluding remarks follow in sections 6 and 7, respectively.

2. Time-slice experiment

The model employed in the time-slice experiment is the ECHAM4 AGCM (e.g., Roeckner et al., 1996a). The model has been developed at the Max-Planck-Institute (MPI) for Meteorology for simulating the global present-day climate and a possible global change in climate due to enhanced emissions of greenhouse gases. It is based on the global forecasting system that is used at European Centre for Medium-Range Weather Forecasting (ECMWF), but several major changes have been made, in particular to the physical parameterizations in order to make the model suitable for climate simulations. Details on the climate statistics of ECHAM4 in its "standard" configuration at a horizontal resolution of T42 (corresponding to 64×128 grid points on a Gaussian grid) and 19 vertical levels can be found in Roeckner et al. (1996a).

In the time-slice experiment we have used ECHAM4 at a horizontal resolution of T106 (corresponding to 160×320 grid points on a Gaussian grid) and 19 vertical levels. In ECHAM4 most of the free parameters in the physical parameterizations are independent of resolution (but note they have been selected at a horizontal resolution of T42) instead of tuning the model by choosing an optimal set of parameters at the respective resolution. Only the parameterizations of a few processes, which have turned out to be extremely scale dependent, have been tuned individually at different horizontal resolutions, such as the parameterizations of gravity wave drag, horizontal diffusion or formation of precipitation in stratiform clouds (e.g., Stendel and Roeckner, 1998). In consequence the high resolution does not automatically reduce all the systematic model errors, since some of the physical parameterizations, which have been tuned at the lower resolution, are possibly scale dependent. Nevertheless the high resolution leads to a more realistic simulation of the present-day climate by ECHAM4 due to the inclusion of a much wider spectrum of spatial scales and, hence, the non-linear interactions between them and a more realistic representation of the topography (Stendel and Roeckner, 1998).

We have performed two simulations with ECHAM4 at the high resolution over a period of 30 years each. These two so-called time-slices have been chosen, so that one 30-year period represents the present-day climate and the other one the climate at a time when the atmospheric concentration of CO_2 has doubled. The first time-slice, which we often will refer to as "TSL_1" hereafter, covers the period 1970 through 1999 and the second one ("TSL_2") the period 2060 through 2089. In each of these time-slices the lower boundary forcing, that are monthly mean values of the SSTs and of the sea-ice extent has been prescribed as obtained

from a climate change simulation performed with a coupled atmosphere-ocean model at low horizontal resolution. Moreover, the temporal evolution of the concentrations of the important greenhouse gases has been prescribed in the same way as in that climate change simulation (see below). Further details on the experimental design of our time-slice experiment are given in May (1999), and a thorough discussion of the changes in the mean climate inferred from these two time-slices can be found therein as well as in May and Roeckner (2000).

The climate change experiment has been performed at MPI. The coupled atmosphere-ocean model consists of the ECHAM4 AGCM at a horizontal resolution of T42 and 19 vertical levels and an extension (level 3) of the OPYC ocean model (Oberhuber, 1993) including a sea-ice model. OPYC has 11 layers and a varying horizontal resolution: poleward of 36° latitude the resolution is identical to that of the low resolution AGCM, that is circa 2.8°. At low latitudes, the meridional grid spacing is gradually decreased down to 0.5° at the equator in order to allow for a better representation of the equatorial wave guide in the model and, hence, the ENSO-phenomenon. Roeckner at al. (1996b) showed that this coupled atmosphere-ocean model actually was able to capture many features of the observed interannual variability of the SSTs in the tropical Pacific. This included not only the amplitude, lifetime and frequency of occurrence of El Niño events, but also the phase-locking of the SST-anomalies and the annual cycle. The model components are coupled quasi-synchronously and exchange information once daily. Annual mean flux-adjustments of heat and freshwater have been estimated from a 100-year spinup of the coupled model. For further details on the coupling technique and the performance of the model we refer to Roeckner at al. (1996b) and Bacher et al. (1998).

This coupled model has been used for a control experiment and for three different time-dependent forcing experiments, which are thoroughly described in Roeckner et al. (1999). At the time, when we decided to perform our time-slice experiment, only the greenhouse gas experiment covering the period 1860 through 2100 (referred to as “GHG” in Roeckner et al. (1999)) was available, so that we could only use this particular climate change experiment for extracting the boundary forcing for our time-slice experiment.

In that climate change simulation the concentrations of various gases have been prescribed as a function of time: the greenhouse gases CO_2, CH_4, N_2O and several industrial gases such as chlorofluorocarbons (CFC-11, 12, 113, 114, 115), hydrochlorofluorocarbons (HCFC-22, 123, 141b), hydrochlorocarbons (HFC-125, 134a, 152a), carbon tetrachloride

(CCl_4) and methylchloroform (CH_3CCl_3). From 1860 to 1990 the annual mean concentrations of these gases have been prescribed as observed and after 1990 according to the scenario IS92a (Houghton et al., 1992). In case of the industrial gases the IS92a-scenario has been updated to be consistent with a "Copenhagen-like" emission scenario (Houghton et al., 1996). This time-dependent or "transient" forcing experiment has been initialized at year 100 of the control run of the coupled model, nominally year 1860 in the transient experiment. In the control run the concentrations of the greenhouse gases (CO_2, CH_4 and N_2O) have been prescribed as observed in 1990 rather than pre-industrial values, and present-day observations have been used for the ocean spinup and for deriving the flux adjustment (Bacher et al., 1998). In consequence the climate in the control run and, hence, the initial state of the transient experiment corresponds to modern rather than the pre-industrial times. Therefore in GHG the initial shift in the concentrations of the greenhouse gases had to be taken into account by enhancing the observed/anticipated concentrations in an appropriate way (see Roeckner at al. (1999) for further details on this procedure).

3. Detection of tropical cyclones

In order to detect tropical cyclones (usually referred to as "TCs" in the following) we apply a number of objective criteria, which are based on dynamical and physical principles obtained from observations as in Walsh (1997), namely

1. The relative vorticity at 850 hpa must exceed a threshold VORTMIN (11×10^{-5} s^{-1});
2. there must be a closed pressure minimum within a certain distance of a point satisfying condition 1; this minimum pressure is taken as the centre of the storm;
3. the wind speed in 10 m must exceed a threshold W10MIN (14 m/s);
4. the total tropospheric temperature anomaly must exceed a threshold TTOT (2 °C);
5. the mean wind speed around the centre of the storm at 850 hPa must be higher than at 300 hPa;
6. the temperature anomaly at the centre of the storm at 300 hPa must be greater than at 850 hPa.

In addition to Walsh (1997) we impose that

7. the minimum duration of the event is 1.5 days

in order to exclude spurious developments in the extratropics (B95). We have applied these detection criteria to the respective meteorological variables originating from the time-slice experiment twice daily (00 and 12 UTC).

We have chosen the threshold values for the meteorological variables in the different detection criteria. i.e., VORTMIN, W10MIN and TTOT, respectively, based on the findings by Walsh (1997). In his study he specified these values, so that he was able to objectively identify TCs in the ECMWF operational analyses in an optimum way, that means obtaining the best agreement with observations. These analyses had the same horizontal resolution as our time-slice experiment, that is T106. Walsh (1997) actually found that the number of vortices detected in the analyses was sensitive to relatively small variations in these threshold values. These thresholds differ somewhat from those chosen in B95 for W10MIN (14 vs. 15 m/s) and for TTOT (2 vs. 3 °C), but considerably for VORTMIN (11×10^{-5} vs. 3.5×10^{-5} s^{-1}). Walsh (1997) found a pronounced sensitivity of the number of detected TCs to the value of W10MIN, less pronounced sensitivity to the value for TTOT and little sensitivity to the choice of VORTMIN.

An important difference to B95 is the calculation of the temperature anomaly used in criteria no. 4 and no. 6. We use a band of 2 grid points south and north of the pressure minimum and 13 grid points to the east end west, that are a total of 5×27 grid points, while in B95 a smaller area of 7×7 grid points was chosen. By this the anomaly test (criterion no. 4) becomes less sensitive to the choice of TTOT (Walsh, 1997). In her analysis of TCs in the ECMWF re-analyses Serrano (1997) applied only a small fraction of the criteria listed above. She considered all TCs with maximum surface winds of 34 knots or greater along their tracks, and the movement of the TC centre was checked using either the minimum sea-level pressure or the maximum relative vorticity at 850 hPa. She found that the relative vorticity yielded somewhat better results than the minimum pressure.

4. Present-day climate

In this section we analyse the simulation of TCs in TSL_1, which covers the period 1970 through 1999 and, hence, represents the present-day climate. In Figure 1 the geographical distribution of the TCs that fulfil the criteria described in the preceding section as obtained from this time-slice is shown. We present both the points of cyclogenesis (Fig. 1a) and the storm tracks indicated in a simplified way via a straight line connecting the respective points of cyclogenesis and cyclolysis (Fig. 1b). The different colours indicate the different seasons. According to Figure 1a, the model is capable to simulate TCs in all the regions, where they typically are observed (Gray, 1979). Further, the occurrence of TCs in the model reveals the observed

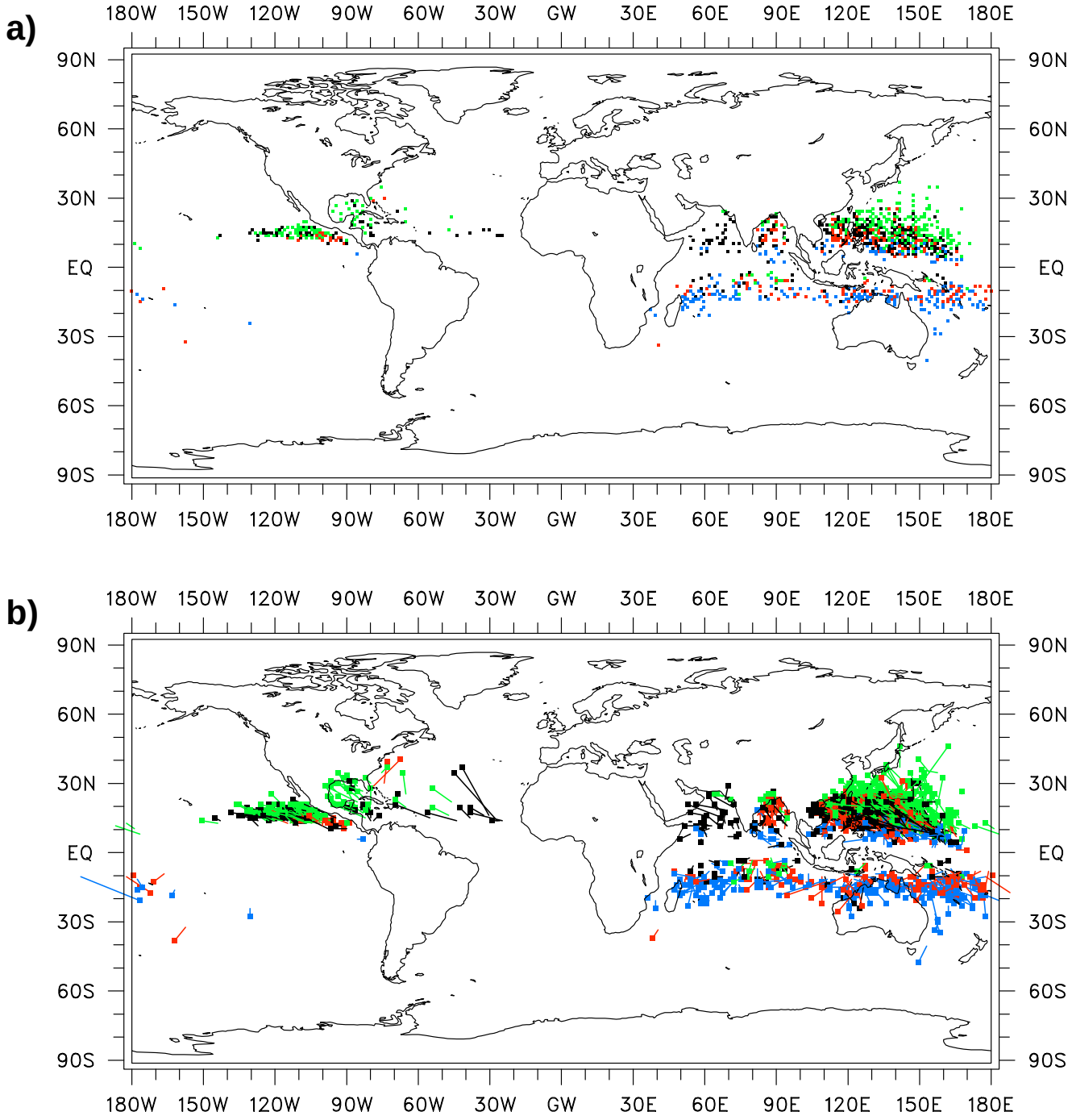

Fig. 1: Locations of tropical storms (i.e., points of cyclogenesis) (a) and simplified tracks of tropical storms (i.e., a straight line connecting the points of cyclogenesis and cyclolysis with the latter one being marked by a square) (b) for TSL_1. The different colours indicate different seasons, namely red: March to May, green: June to August, black: September to November and blue: December to February.

seasonal variation: in the Southern Hemisphere TCs occur in the austral summer (DJF) and austral autumn seasons (MAM), while in the Northern Hemisphere TCs can be found in all seasons (Fig. 1a). In boreal winter (DJF) the occurrence of TCs in the Northern Hemisphere is confined to the Indian and the western Pacific Ocean. The TCs reach their most poleward locations during the respective summer seasons. These seasonal variations can also be identified in Figure 2, which will be discussed in the following paragraph. As to be seen from the cyclone tracks (Fig. 1b), in the Northern Hemisphere the TCs generally move poleward and westward except for DJF. During this season the TCs over the Indian and the western Pacific Ocean move eastward and equatorward, in case they move parallel a circle of longitude. Also in the Southern Hemisphere the TCs generally move poleward, but tend to take a westerly route over the central Indian Ocean and an easterly route over the eastern Indian and the western Pacific Ocean. In agreement with observations (Gray, 1979), the TCs tend to turn back into the eastward direction in their later life stage after they have moved poleward for a number of days. We also find a number of land-falling TCs in our simulation in all regions, but in particular in Australia.

As argued by B95 a certain value of the SSTs, which determines the heat supply from the ocean, is a necessary condition for the development of TCs. In Figure 2 we therefore show both the areas, where the SSTs exceed a value of 26 °C, and the points of cyclogenesis for different seasons. Apparently in our simulation all TCs (there are only very few exceptions) develop in regions, where the SSTs exceed 26 °C. But there are also very large areas, where no TCs develop though the SSTs exceed the threshold of 26 °C. In these areas obviously other factors determining the cyclogenesis are not as favourable as the SSTs, that is the heat supply from the ocean. According to B95, the existence of large-scale convergence in the lower part of the troposphere is another necessary condition for the development of TCs in those areas, where the Coriolis force is strong enough to provide the required convergence. As the areas of large-scale convergence change relatively slowly and the vertical wind shear is weak, the TCs are allowed to develop the essential vertical structure. Furthermore, the tropospheric water vapour content is maintained at a very high level due to the steady large-scale moisture convergence. By this one can, for example, explain the absence of TCs over the southern Atlantic due to the predominant sinking motion enforced by the large-scale convection over equatorial Africa and over western Brazil. The suppression of hurricanes over the northwestern Atlantic during El Niño events can then be related to the compensating sinking motion in that area as a consequence of the eastward position of the area of convergence over the Pacific.

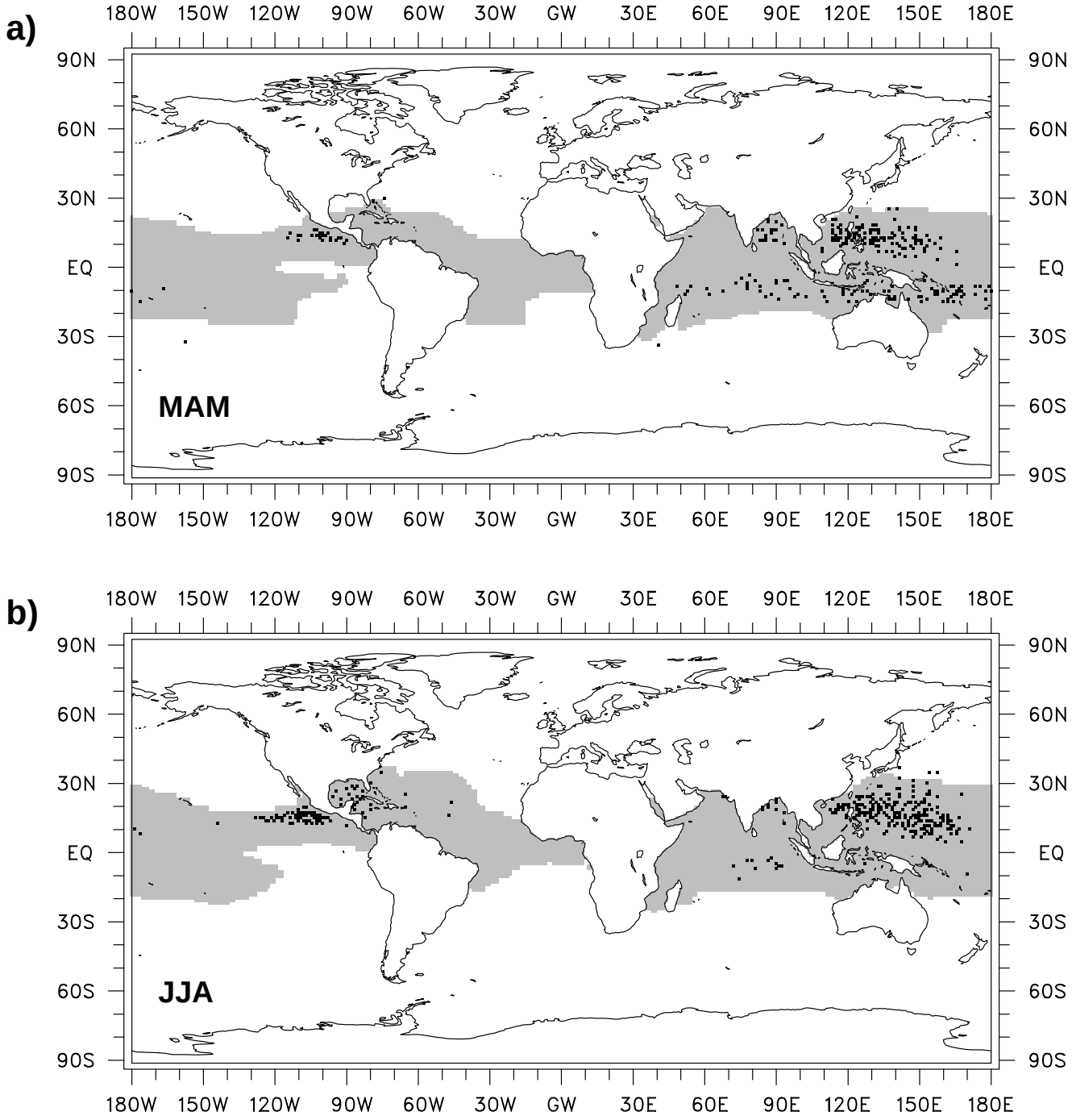

Fig. 2: Locations of tropical storms (i.e., points of cyclogenesis) for TSL_1 in the seasons March to May (a) and July to August (b). Those areas, where the SSTs exceed 26 °C in the respective season, are marked by the shading.

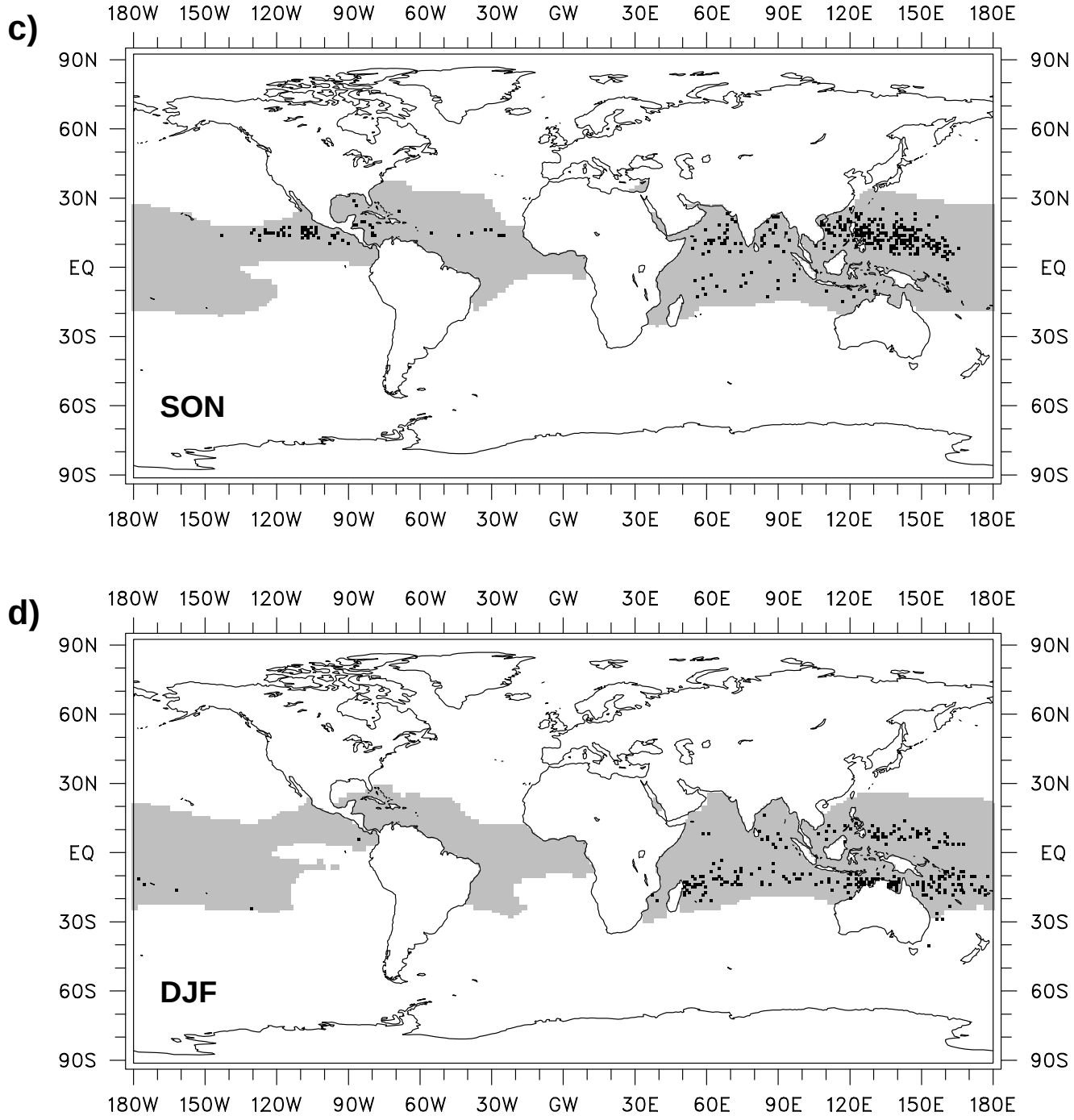

Fig. 2: **(continued)** Locations of tropical storms (i.e., points of cyclogenesis) for TSL_1 in the seasons September to November (c) and December to February (d). Those areas, where the SSTs exceed 26 °C in the respective season, are marked by the shading.

When comparing the total number of TCs in the simulation with observations (Gray, 1979) we have, however, to realize that the model does not produce a realistic number of TCs in any region (Fig. 3). In general the number of TCs is underestimated by 40 to 50% (Table 1). Over the northwestern Atlantic our simulation reveals only about 20% of the observed number of TCs, and only over the northwestern Pacific produces the model a realistic number of TCs (ca. 84%). Considering the very wide range of the numbers of TCs in individual years, we find that only in those years, when the maximum numbers of TCs occur in the simulation in a particular region, the model simulates about the same number of TCs as the observations reveal on average. In some regions, i.e., over the northwestern Atlantic and the northeastern Pacific Ocean as well as over the southern Indian and the southern Pacific Ocean, the model does not simulate any TC at all during individual years. This is, however, not the case in the observations. The variations from year to year in the different regions as seen in the simulation are in general of the same magnitude as in the observations.

Considering individual months (Fig. 4) we find the most severe underestimation of TCs by the model in those periods, when most of the TCs typically occur, that are the periods July to October in the Northern (Fig. 4a) and December to April in the Southern Hemisphere (Fig. 4b). In the respective months the model produces only about 40 to 50% of the TCs revealed in the observations (Table 2). But the model produces relatively many TCs at those times of the year, when the TC activity is weak, i.e., in the periods January to May in the Northern and June to September in the Southern Hemisphere. In the Northern Hemisphere the annual cycle as obtained from the simulation is actually quite different than in the observations (Gray, 1979), since the pronounced maximum between July and October does not appear (Fig. 4a). Further, the model simulates most TCs in July and a rather large number in May. This feature is mainly related to the annual cycle over the northwestern Pacific (not shown), where the largest fraction of the TCs in the Northern Hemisphere can be found in our simulation as well as in the observations (Fig. 3). In the Southern Hemisphere, on the other hand, the variation of the number of TCs in the course of the year as obtained from the simulation is very similar to the observations (Fig. 4b).

We have analysed the intensity of the TCs that have been identified in TSL_1 considering both the minimum pressure and the maximum wind speed in 10 m that the individual TCs obtain during their lifetime as a measure of the TCs' strength. According to these estimates of the intensity we have divided the TCs into 7 categories, namely

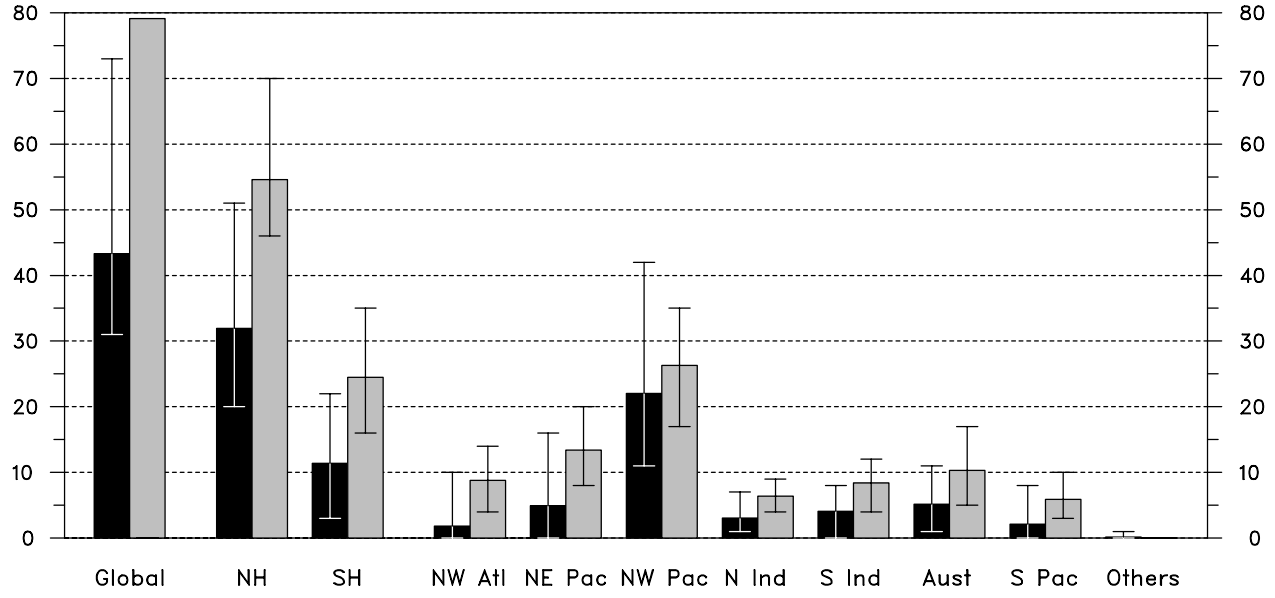

Fig. 3: Numbers of tropical storms for TSL_1 (black columns) and for observations (Gray, 1979) (grey columns) distinguishing between different areas (Bengtsson et al., 1995). Also the maximum and the minimum numbers of storms occurring in individual years in the respective areas and the respective data sets (bars). Units are [storms/year].

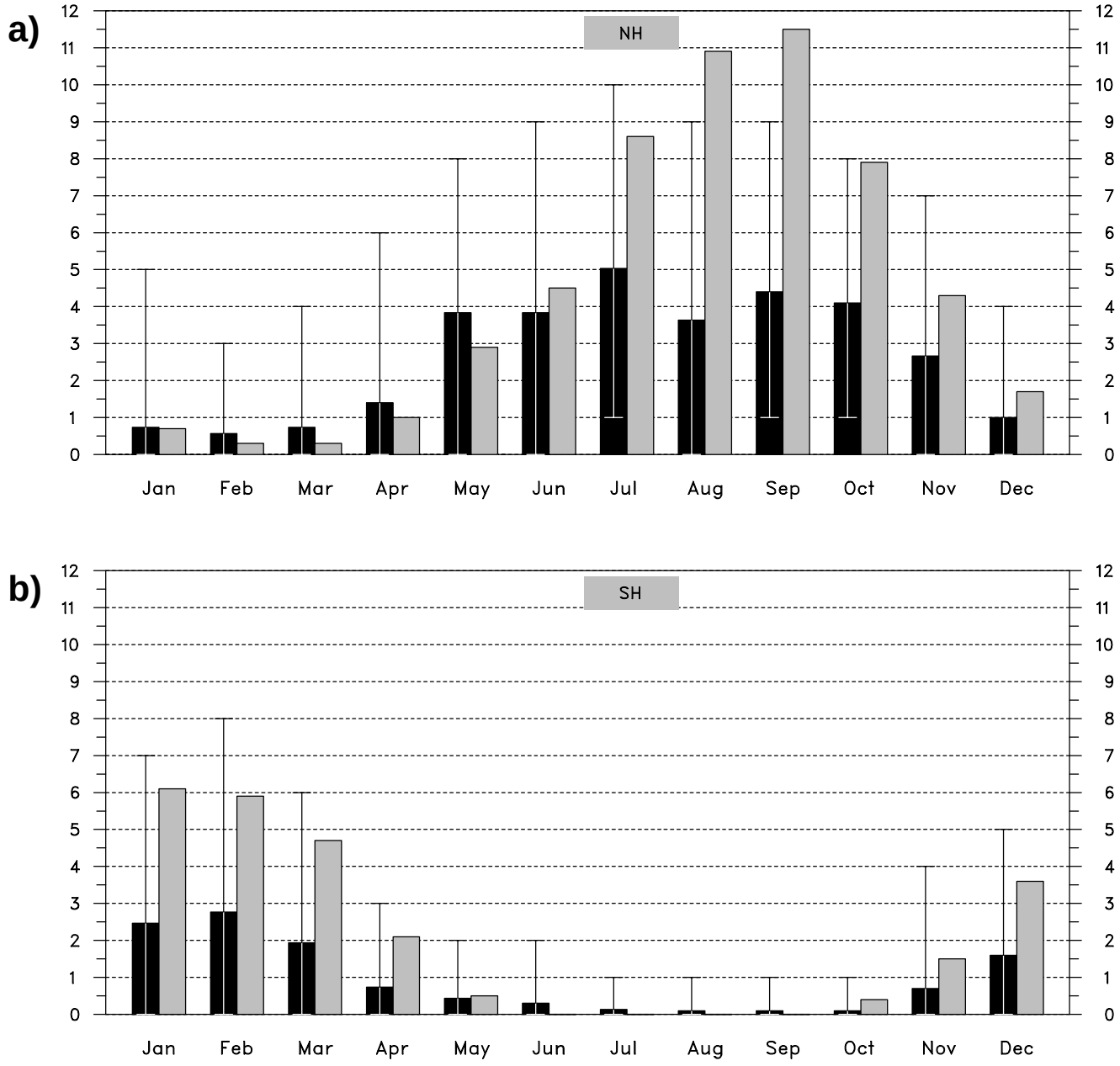

Fig. 4: Numbers of tropical storms for TSL_1 (black columns) and for observations (Gray, 1979) (grey columns) distinguishing between different months for the Northern (a) and the Southern Hemisphere (b). Also the maximum and the minimum numbers of storms occurring in individual years in the respective months for TSL_1 (bars). Units are [storms/year].

Class 1: PRMIN ≤ 980 hPa and W10MAX ≥ 26 m/s;
Class 2: 980 hPa < PRMIN ≤ 985 hPa and 26 m/s > W10MAX ≥ 24 m/s;
Class 3: 985 hPa < PRMIN ≤ 990 hPa and 24 m/s > W10MAX ≥ 22 m/s;
Class 4: 990 hPa < PRMIN ≤ 995 hPa and 22 m/s > W10MAX ≥ 20 m/s;
Class 5: 995 hPa < PRMIN ≤ 1000 hPa and 20 m/s > W10MAX ≥ 18 m/s;
Class 6: 1000 hPa < PRMIN ≤ 1005 hPa and 18 m/s > W10MAX ≥ 16m/s; and
Class 7: PRMIN > 1005 hPa and W10MAX < 16 m/s.

In Figure 5 we show the frequency distributions of the intensities of the TCs for the different categories distinguishing between the global estimates and the values for the two hemispheres. According to this, the TCs simulated by the model are unrealistically weak. Most of the TCs fall into the classes 5 and 6, that is they have maximum wind speeds between 16 and 20 m/s and a minimum pressure between 995 and 1005 hPa. Only in a few cases the pressure drops below 990 hPa and the wind speed exceeds 22 m/s (classes 1-3). As a consequence, the simulation does not reveal any hurricanes or typhoons with wind speeds above 33 m/s (Neumann, 1993). This holds for both the Northern and the Southern Hemisphere and also for the various regions referred to in Figure 3 (not shown).

This result is quite different from the finding by B95, who in a similar model experiment were able to obtain quite realistic wind speeds. The wind speeds were about twice as high as in our simulation, and extremes of more than 50 m/s were reached. In their experiment B95 used the ECHAM3 atmospheric GCM at a horizontal resolution of T106, which is the same resolution as in our time-slice experiment. But the ECHAM4 model we have used here has undergone major changes in both the numerical methods and the physical parameterizations compared to ECHAM3, the previous version of the ECHAM model (Roeckner et al., 1996a). These include a semi-Lagrangian transport scheme, a new radiation scheme with modifications concerning the water vapour continuum, cloud optical properties and greenhouse gases, a new formulation of the vertical diffusion coefficients as functions of the turbulent kinetic energy as well as a new closure of for deep convection based on convective instability instead of moisture convergence. Minor changes concern the parameterizations of horizontal diffusion, stratiform clouds and land surface processes. Roeckner et al. (1996a) found, for instance, that at a horizontal resolution of T42 the model's systematic errors in the tropospheric temperature and zonal wind fields were generally smaller in ECHAM4 except in the tropics, where the overestimation of Walker-type circulations in the equatorial band is more pronounced in ECHAM4,

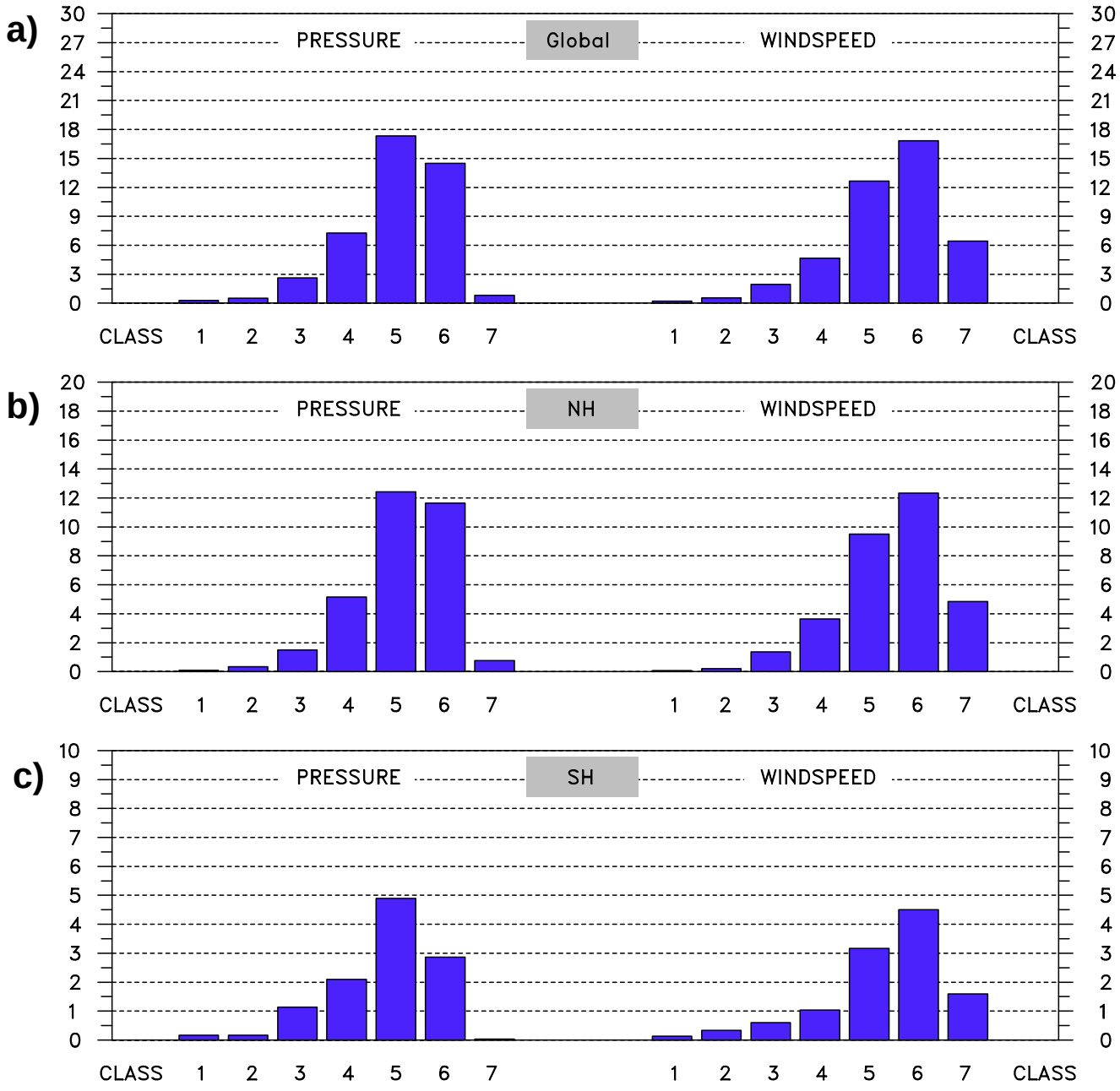

Fig. 5: Intensities of tropical storms for TSL_1 defined via the minimum pressure as well as via the maximum wind speed in 10 m distinguishing between the entire globe (a), the Northern (b) and the Southern Hemisphere (c). For the definition of the different classes see the text (section 4). Units are [storms/ year].

and the simulation of the Indian summer monsoon is less realistic. Considering the simulation of TCs the aforementioned changes in the ECHAM model have apparently affected the GCM in a very negative way. This can be either certain aspects of the large-scale circulation affecting the atmospheric static stability or the vertical wind shear or local processes affecting the convergence of the atmospheric moisture fluxes, the release of latent heat or the interaction with the ocean, which all have an impact on the development and the strength of TCs (e.g., Holland, 1997; Shen et al., 2000). The discrepancy between the two versions of the ECHAM model clearly shows, how crucially the simulation of TCs depends on the physical parameterizations of the respective GCM.

The studies by B95 and B96 were based on relatively short periods of data, i.e., 5 years for each time-slice. As pointed out by the authors these were rather short periods of data given the large interannual variations in the occurrence of TCs, adding uncertainty to some of the results obtained in these studies. In Figure 6 we therefore take a look at the frequency of TCs for the 6 consecutive 5-year periods covering the 30 years of our time-slice. According to this, we find rather large variations between the 6 periods. This is even the case for the global values, where we find a range of about 22% of the average value for the entire 30 years. These variations are related to both the Northern and the Southern Hemisphere with a range of approximately 29% and 26%, respectively. Different to the Northern Hemisphere, one can obtain an upward trend over the 30-year period in the Southern Hemisphere. This is, however, quite intriguing, since we find rather large variations and not such an upward trend in the individual regions in the Southern Hemisphere (not shown).

5. Future climate

In this section we analyse the simulation of TCs in TSL_2 representing the future climate and assess the possible changes in the frequency and intensity of TCs in a warmer climate. TSL_2 covers the period 2060 through 2089. In Figure 7 we show the geographical distribution of TCs, that are the points of cyclogenesis as obtained from TSL_2. According to this, in the future climate TCs occur in the same regions, where they typically occur at the present time. In particular, the distribution does not give any indication of TCs developing at larger distances from the equator than in TSL_1 (see Fig. 1a) though the SSTs are generally warmer in the future climate (see Fig. 8; to be discussed in the following paragraph). Compared to the present-day climate (see Fig. 1a) there seems to be a general tendency of less TCs in a warmer climate,

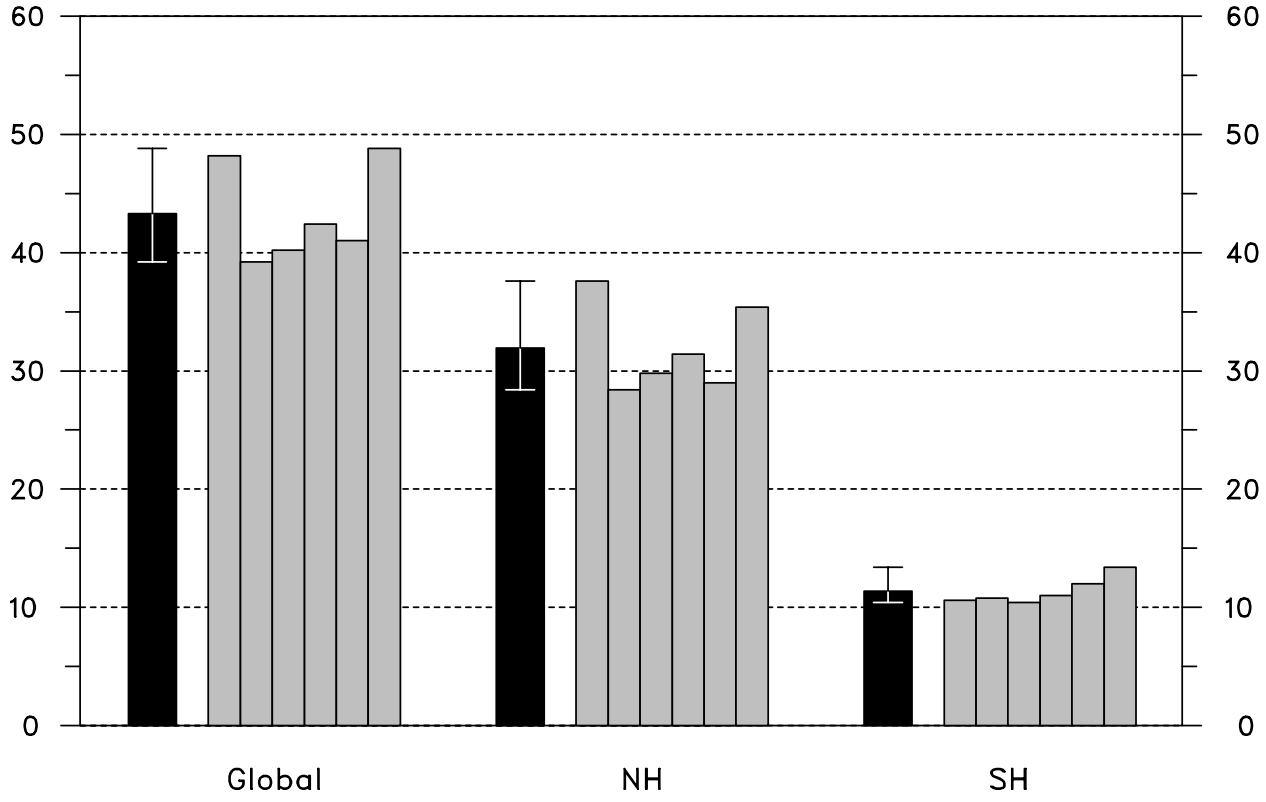

Fig. 6: Numbers of tropical storms for TSL_1 (black columns) as well as for 6 individual 5-year periods of TSL_1 (grey columns). Also the maximum and the minimum numbers of storms occurring in individual 5-year periods in the respective areas (bars). We distinguish between the entire globe (a), the Northern (b) and the Southern Hemisphere (c). Units are [storms/year].

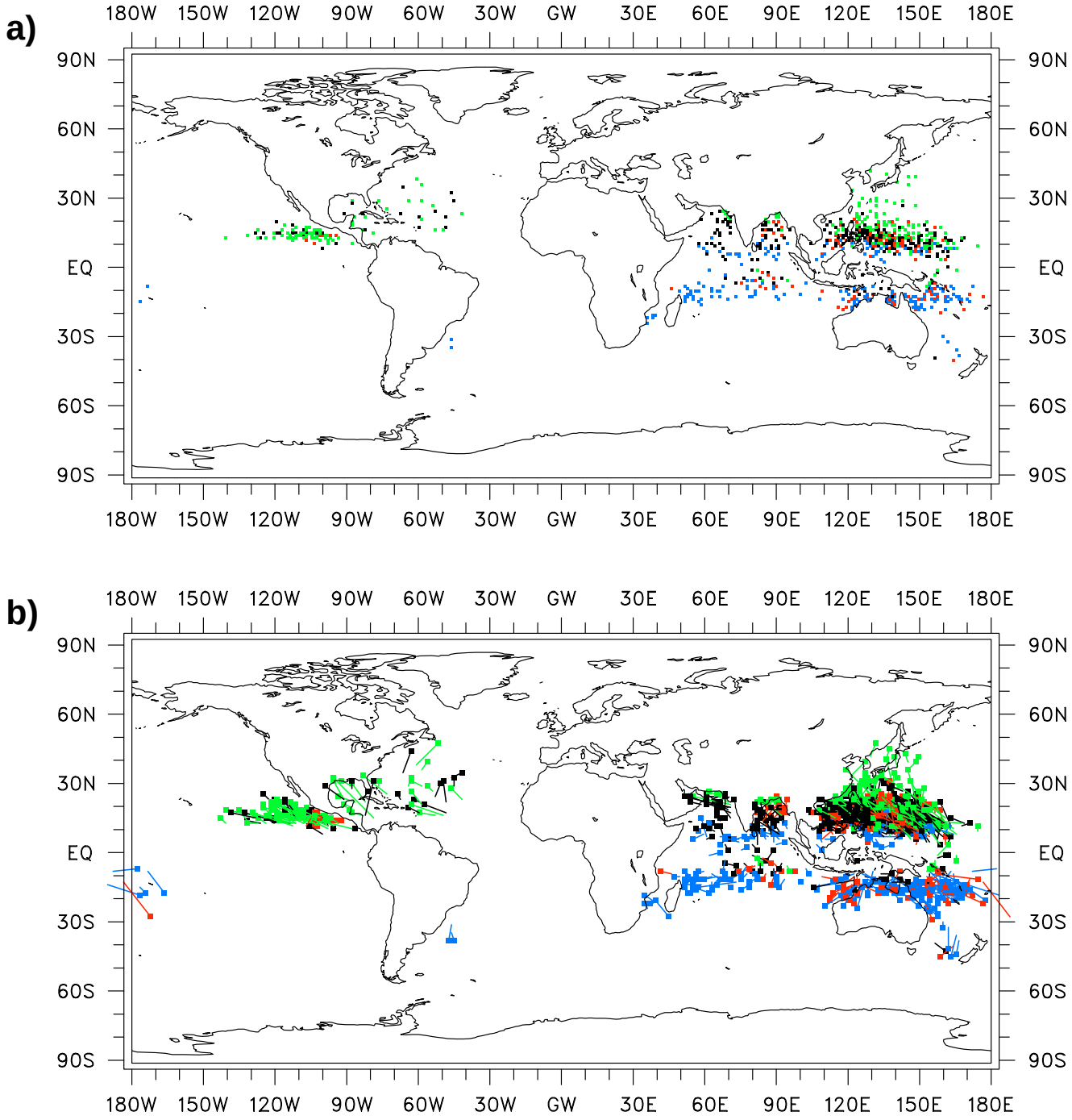

Fig. 7: As Fig.1, but for TSL_2.

especially over the northeastern Pacific and in the Caribbean but also over the northwestern Pacific.

In Figure 8 we show both the points of cyclogenesis and the areas, where the SSTs exceed 28 °C, which is 2 °C higher than in the respective figure for TSL_1 (see Fig. 2), as obtained from TSL_2. Since those areas, where the SSTs exceed 28 and 26 °C, respectively, in the two time-slices roughly correspond to each other, the SSTs in the tropics are approximately 2 °C warmer in TSL_2. And since the TCs develop in roughly the same areas as in the simulation of the present-day climate and, hence, at locations with about 2 °C warmer SSTs, it are apparently the changes in the atmospheric conditions rather than the larger supply of energy, which becomes available at the sea surface, that control the changes in the frequency of TCs in our experiment. Further comparison between the two time-slices reveals in boreal spring (MAM) a clear reduction of the number of TCs in all areas (Figs. 2a and 8a), while for the other seasons such obvious changes cannot be inferred directly from the respective plots.

The statistical analysis of the number of TCs occurring in the two time-slices reveals a reduction of the frequency of TCs in all regions except for the region over the northern Indian Ocean (Fig. 9). On a global scale the reduction is about 23% with a somewhat smaller decrease in the Northern and a somewhat larger reduction in the Southern Hemisphere (Table 4). Considering the individual regions, we find a much more modest reduction in Australia (about 10%). Despite of the general reduction, which TSL_2 reveals in all regions but the northern Indian Ocean, in some years we identify more TCs than the average values obtained from TSL_1. Along with the general reduction of the frequency of TCs goes a reduction of the range for individual years. In particular the upper limit, which indicates the maximum number of TCs in a particular year, is lower then in TSL_1.

These results confirm by and large the main conclusion from B96 that the frequency of TCs decreases in a warmer climate. A direct comparison with the results by B96 (Table 4), reveals, however, a couple of important differences. First of all, we find an increase in the TC activity over the northern Indian Ocean, while B96 identified a reduction in this area as well. Further, B96 found a much larger reduction in the Southern than in the Northern Hemisphere, while we obtain about the same magnitude of the decrease in both hemispheres. This discrepancy is related to the considerably stronger reductions in the region over the southern Indian Ocean and in Australia in B96 than in our model experiment (64.1 vs. 35.8% over the southern

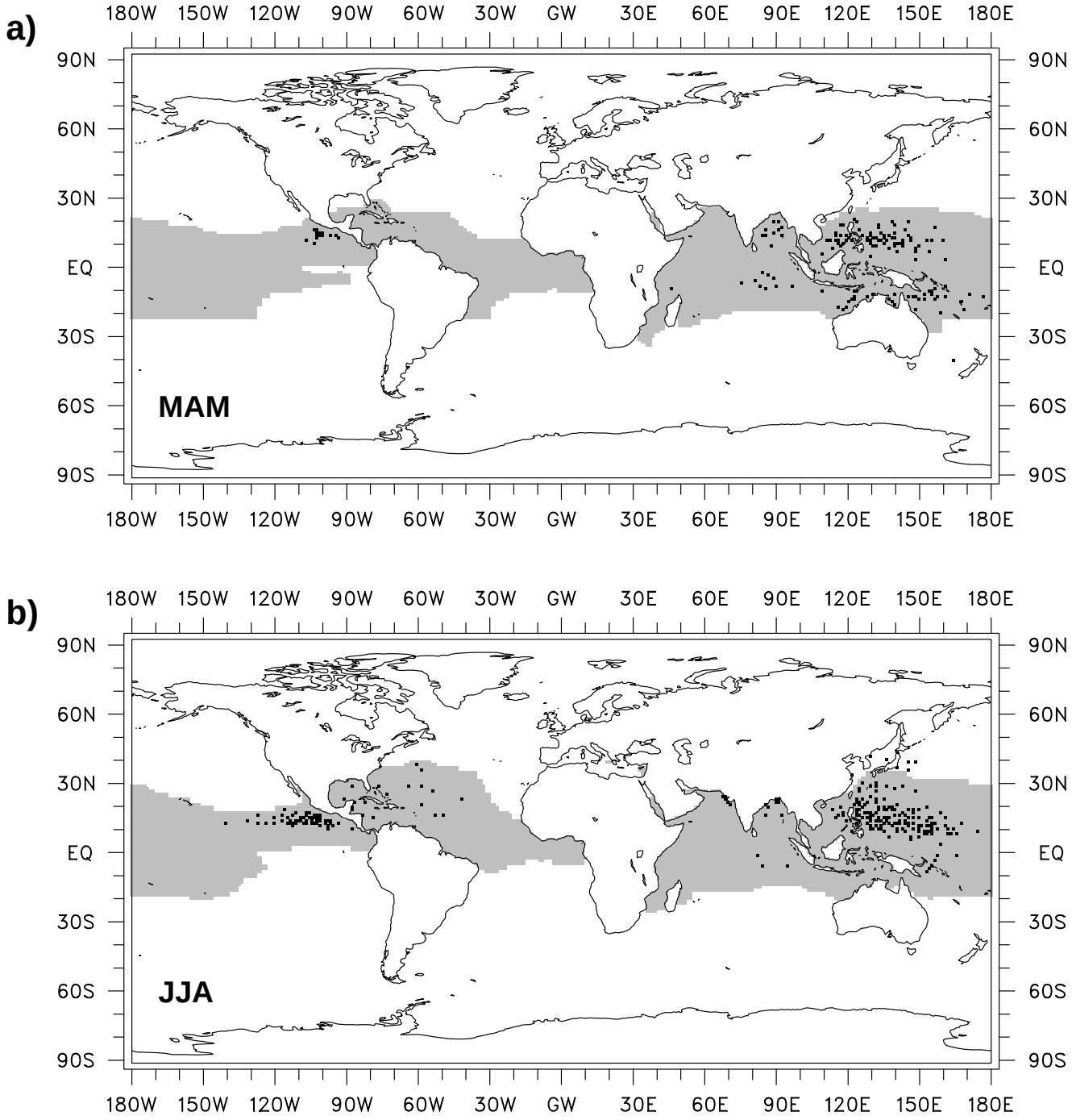

Fig. 8: As Fig. 2, but for TSL_2. Those areas, where the SSTs exceed 28 °C in the respective season, are marked by the shading.

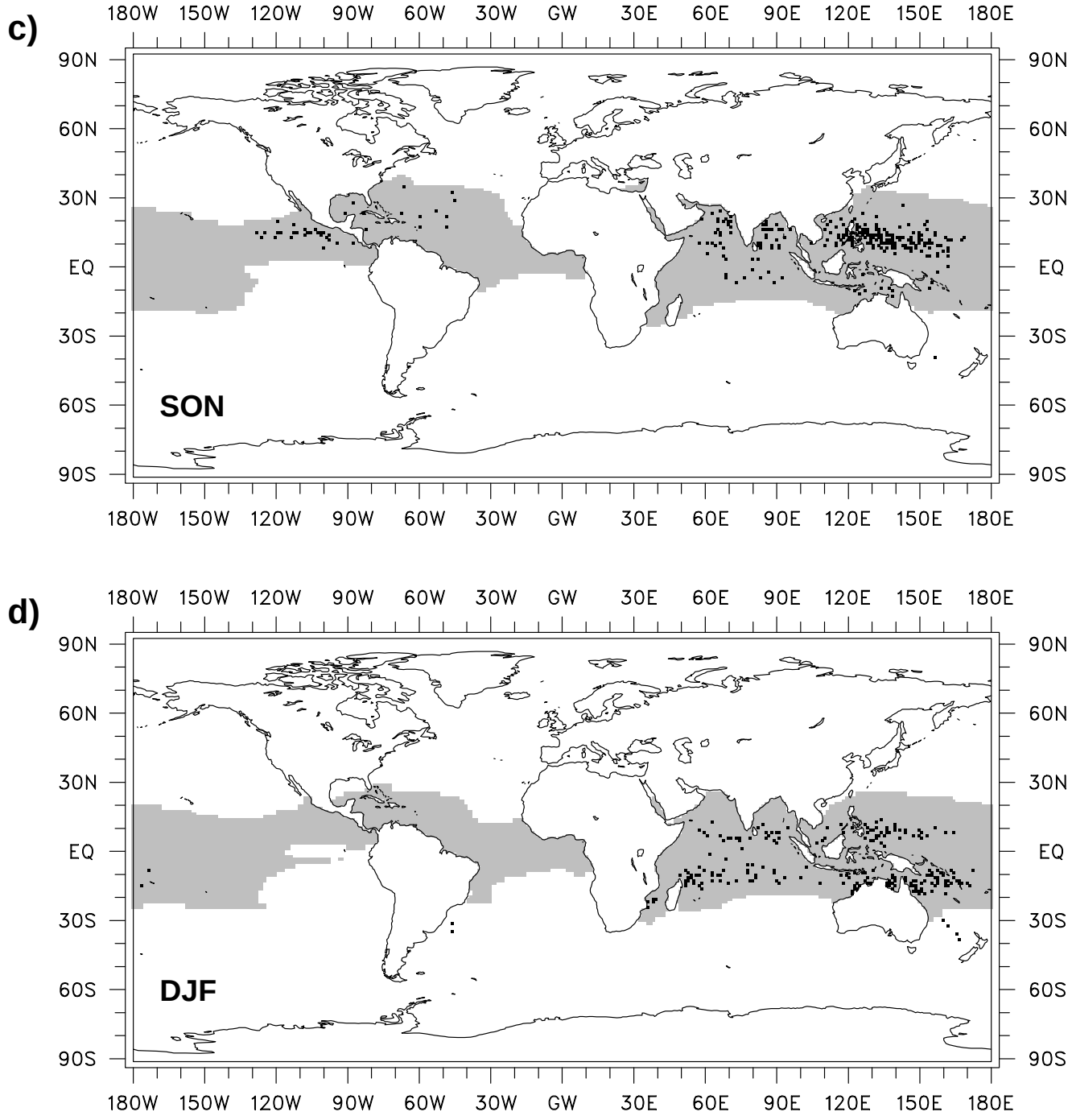

Fig. 8: **(continued)** As Fig. 2, but for TSL_2. Those areas, where the SSTs exceed 28 °C in the respective season, are marked by the shading.

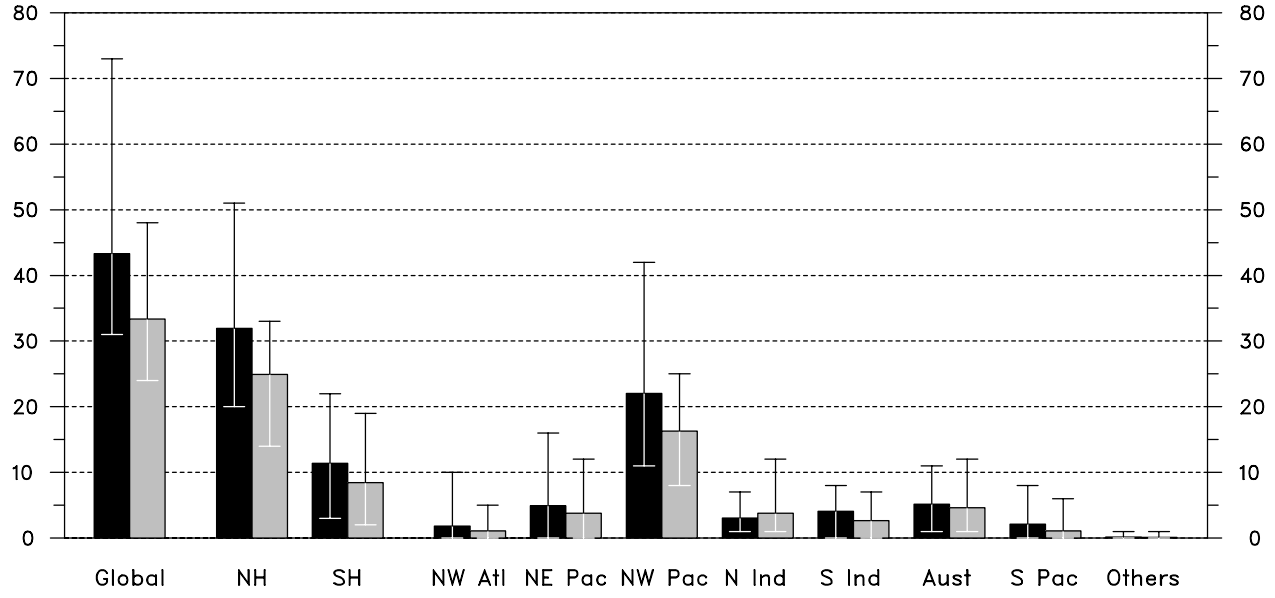

Fig. 9: Numbers of tropical storms for TSL_1 (black columns) and for TSL_2 (grey columns) distinguishing between different areas. Also the maximum and the minimum numbers of storms occurring in individual years in the respective areas and the respective data sets (bars). Units are [storms/year].

Indian Ocean and 53.2 vs. 9.7% in Australia). These are, however, the regions, where most of the TCs in the Southern Hemisphere occur (see Fig. 2).

In the Northern Hemisphere the decrease in the frequency of TCs is present during all months but December (Fig. 10a), when the frequency increases by about 57% (Table 5). Further, the reduction is rather strong (more than 40%) in spring and early summer (March to June) and relatively weak in autumn (September to November). The annual cycle is generally similar in the two time-slices with a maximum in July and rather large values in September and October (Fig. 10a). In the region over the northwestern Pacific (Fig. 10c) both the variation in the course of the year and the magnitude of the reduction in the number of TCs are very similar to the behaviour in entire Northern Hemisphere. Also the increase in December occurs, though to a considerably smaller extent (approximately 17%). Over the northern Indian Ocean (Fig. 10d), on the other hand, the frequency of TCs increases during most of the monsoon season, that is in June, August and September, which may be related to a possible intensification of the Indian summer monsoon in the future climate. According to Annamalai et al. (1999) the occurrence of tropical cyclones over the Bay of Bengal is affected by the strength of the Indian summer monsoon with the tropical cyclones penetrating deep into the continent during very strong monsoon years. In particular in the later stage of the monsoon considerably more TCs occur in the future climate, in August we actually can identify a three-doubling in the number of TCs and in September an increase by a factor of about 2.4 (Table 5). To a large extent the increase during the monsoon season occurs, however, over the Arabian Sea with a ratio of 280% and only to a much smaller extent over the Bay of Bengal (114%). Also during the boreal winter season, that is the period November to January we find such strong increases in the frequency of TCs in that area. In that season many more TCs can be identified over the central Indian Ocean in TSL_2 (see Fig. 8d) than for TSL_1 (see Fig. 2d). In the Southern Hemisphere (Fig. 10b), on the other hand, the frequency of TCs is reduced in virtually all months with a small reduction at the beginning of the TC season (December and January) and a rather large reduction (30 to 40%) at the end (February and March) (Table 5).

When we consider the absolute numbers of TCs identified in the two time-slices, we find that the frequency distributions of the TCs' intensities by and large reflect the reduction of the number of TCs in TSL_2 (Fig. 11). In the Northern Hemisphere and, hence, on a global scale we obtain only in class 7 (wind speed below 16 m/s) more TCs in TSL_2 than in TSL_1. In the area over the northern Indian Ocean, on the other hand, there are more TCs in virtually all of the

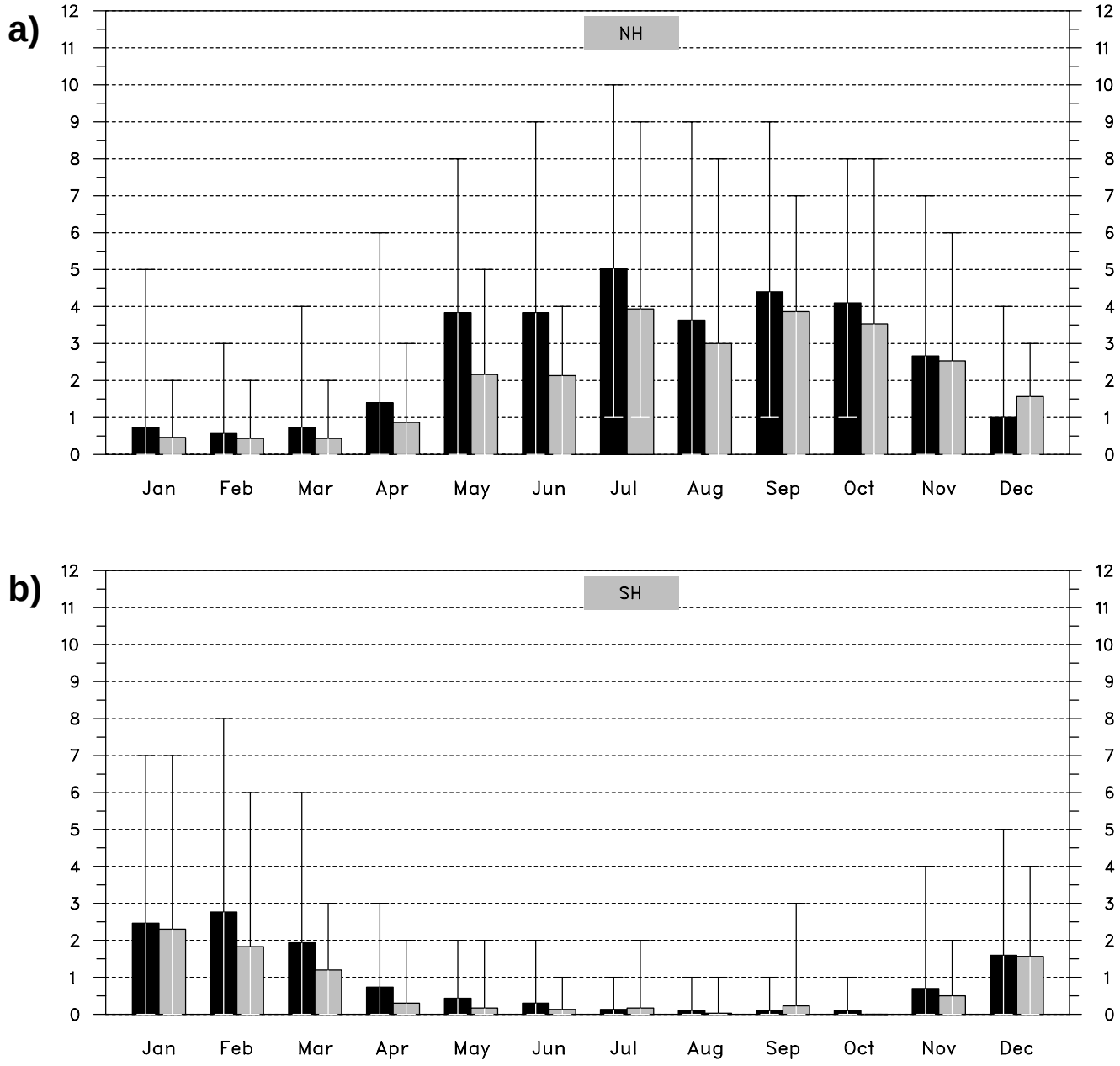

Fig. 10: Numbers of tropical storms for TSL_1 (black columns) and for TSL_2 (grey columns) distinguishing between different months for the Northern (a) and the Southern Hemisphere (b). Also the maximum and the minimum numbers of storms occurring in individual years in the respective months and the respective data sets (bars). Units are [storms/year].

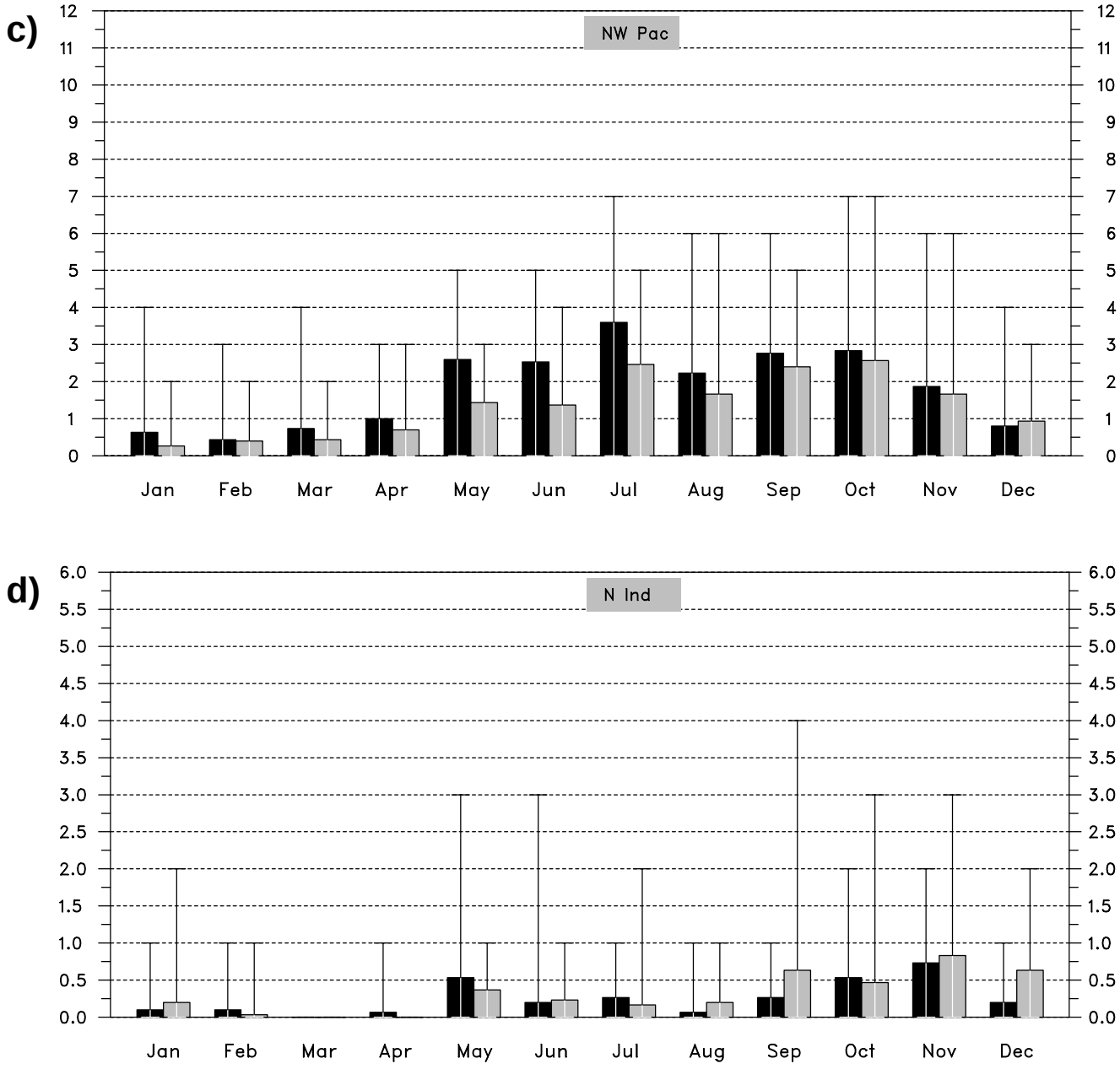

Fig. 10: **(continued)** Numbers of tropical storms for TSL_1 (black columns) and for TSL_2 (grey columns) distinguishing between different months for the northwestern Pacific (c) and the northern Indian Ocean (d). Also the maximum and the minimum numbers of storms occurring in individual years in the respective months and the respective data sets (bars). Units are [storms/year].

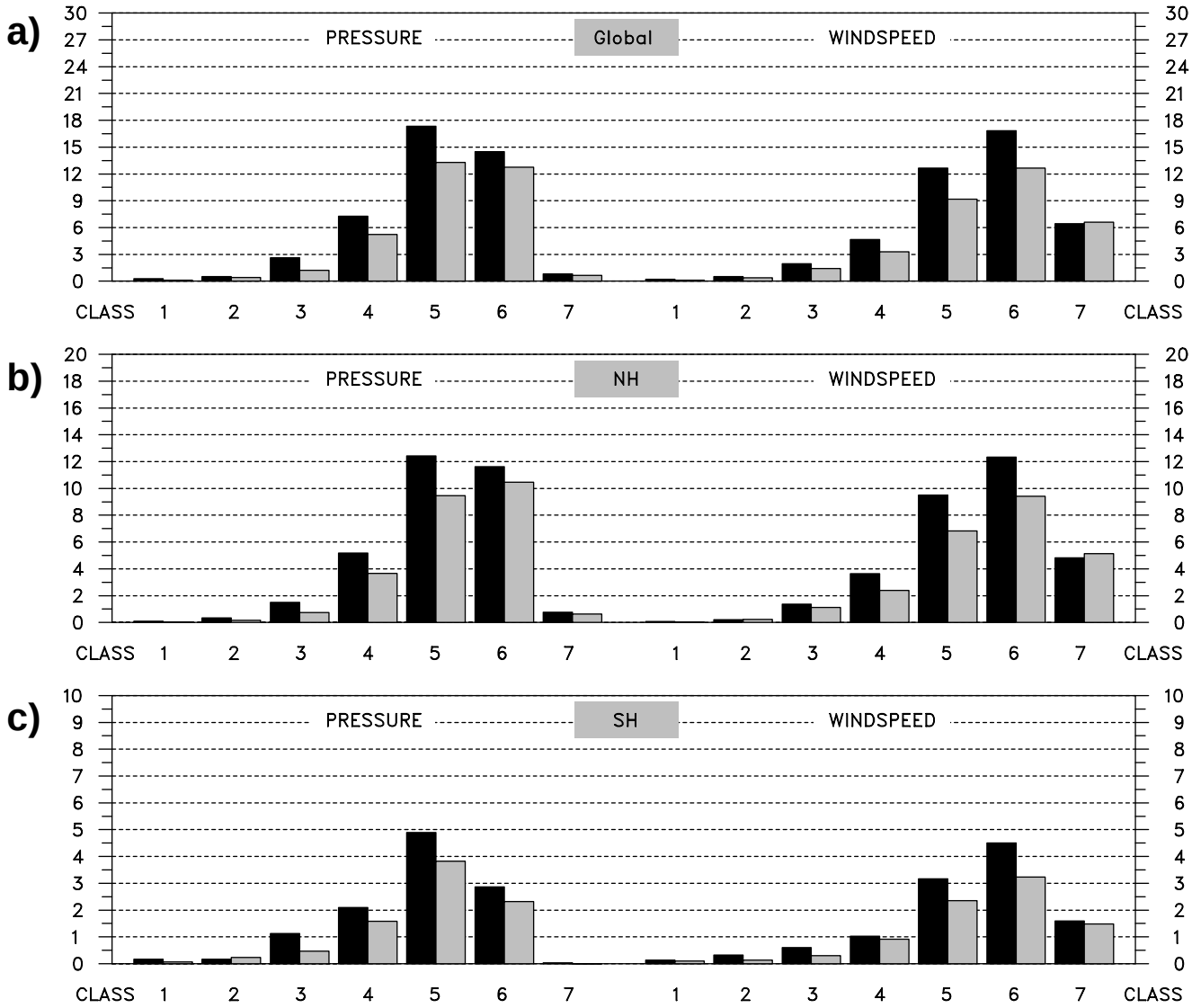

Fig. 11: Intensities of tropical storms for TSL_1 (black columns) and TSL_2 (grey columns) defined via the minimum pressure as well as via the maximum wind speed in 10 m distinguishing between the entire globe (a), the Northern (b) and the Southern Hemisphere (c). For the definition of the different classes see the text (section 4). Units are [storms/year].

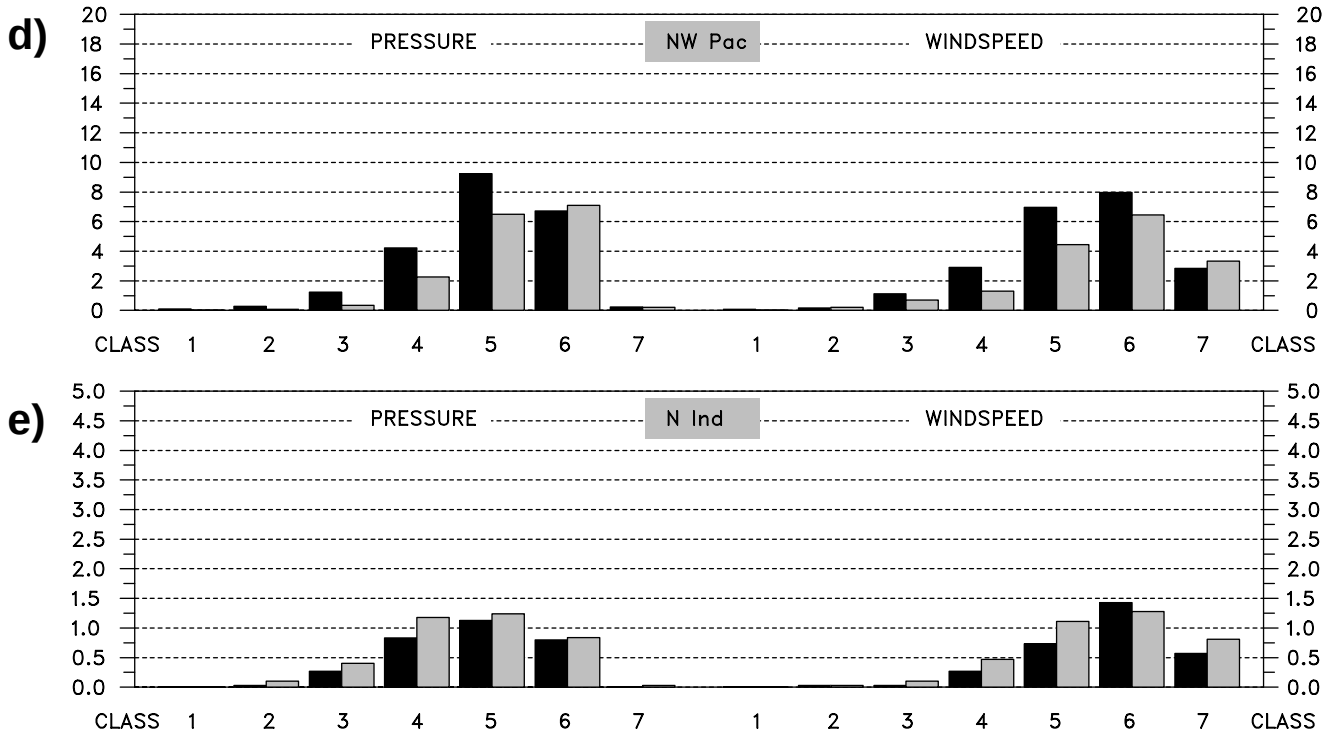

Fig. 11: **(continued)** Intensities of tropical storms for TSL_1 (black column) and TSL_2 (grey column) defined via the minimum pressure as well as via the maximum wind speed in 10 m distinguishing between the entire northwestern Pacific (d) and the northern Indian Ocean (e). For the definition of the different classes see the text (section 4). Units are [storms/year].

different categories. For the weakest TCs (classes 6 and 7) we find, however, a different behaviour depending on whether we consider the minimum pressure or the maximum wind speed as a measure of the TCs' intensities. For the wind speed we obtain a rather large increase in class 7 and a reduction in class 6, but for the pressure a relatively small increase in both categories. This tendency is quite robust, since it also occurs in the region over the northwestern Pacific as well as in the Southern Hemisphere.

When we, however, take the changes in the absolute numbers of TCs between the two time-slices into account, we can assess changes in the intensity of TCs in a warmer climate (Fig. 12). On a global scale as well as in the two hemispheres there are more relatively weak (class 6 for the pressure and class 7 for the wind speed) and less rather intense TCs (classes 1-5 for the pressure and classes 1-6 for the wind speed). This is also the case over the northwestern Pacific, though in this area more TCs fall into class 6 for the wind speed. In the region over the northern Indian Ocean the situation is quite different. There we find more intense and less relatively weak TCs in the future climate, since for the pressure there are more TCs in classes 2 to 4 and for the wind speed in classes 3 to 5.

Also in TSL_2 we find considerable variations between the 6 consecutive 5-year periods of the time-slice (Fig. 13). On a global scale the estimates of the range have about the same magnitude for the two time-slices (Table 3), but if we take a look at the two hemispheres separately we find a much larger (about 2 times) range between the different periods in TSL_2 for the Southern Hemisphere. On a global scale, in the Northern Hemisphere as well as in the region over the northwestern Pacific the range between the different periods is of about the same magnitude as the change associated with the global warming (see Table 4), while in the Southern Hemisphere, where about 1/4 of the TCs occur, as well as in the other individual regions the range is considerably larger than the change in the frequency of the TCs.

6. Discussion

Though the SSTs in the tropical regions have warmed by about 2 °C, the time-slice experiment predicts a general reduction of the number of TCs in the future climate. Apparently the changes in the large-scale circulation are unfavourable for the development of TCs, while the increased temperatures at the surface are favourable. Therefore we will discuss the changes in some of the relevant aspects of the large-scale circulation in this section. We concentrate on

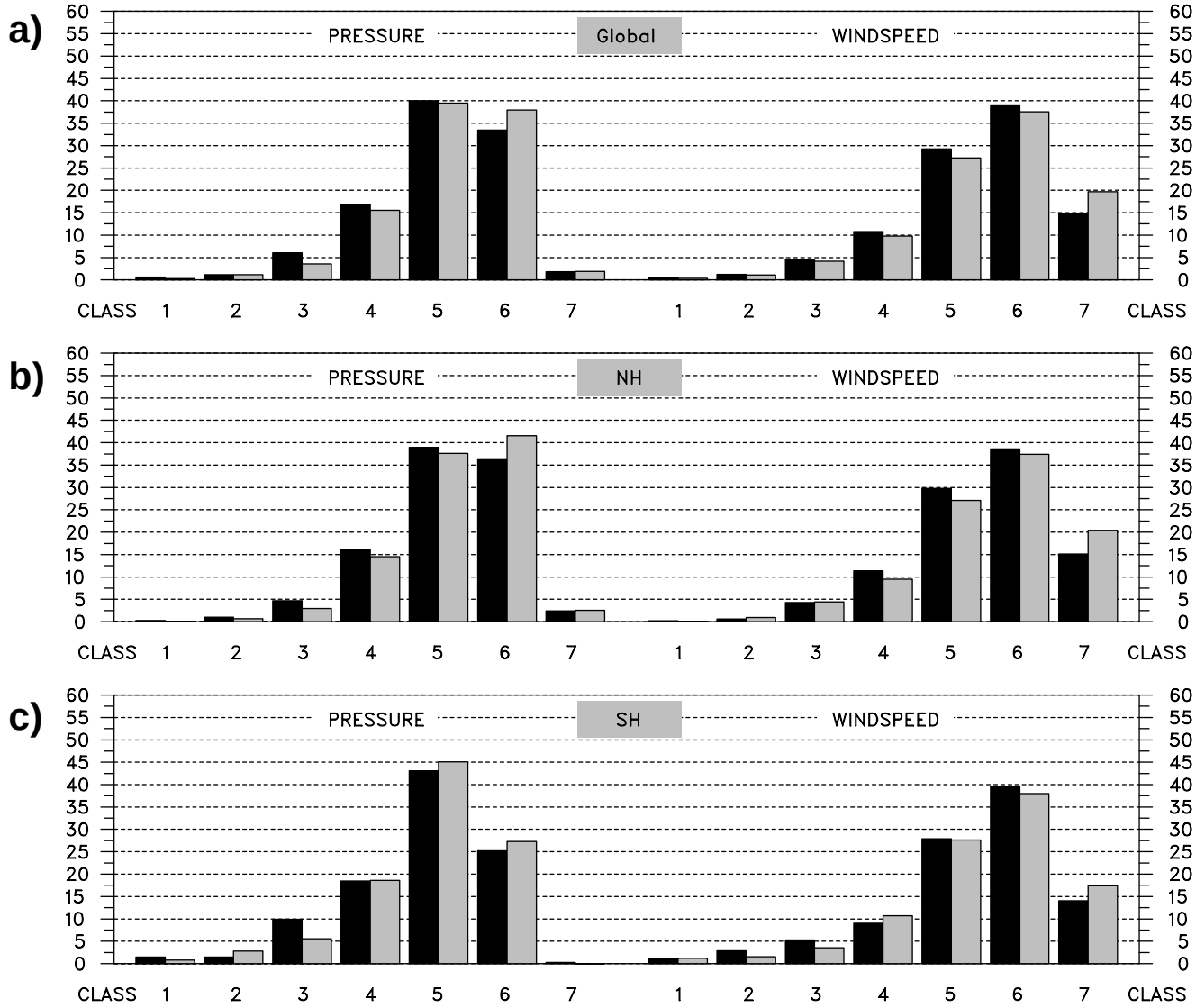

Fig. 12: Intensities of tropical storms for TSL_1 (black columns) and TSL_2 (grey columns) defined via the minimum pressure as well as via the maximum wind speed in 10 m distinguishing between the entire globe (a), the Northern (b) and the Southern Hemisphere (c). The estimates have been obtained by dividing the numbers of storms in each class by the overall numbers of storms for the respective areas and the respective data sets. For the definition of the different classes see the text (section 4). Units are [%].

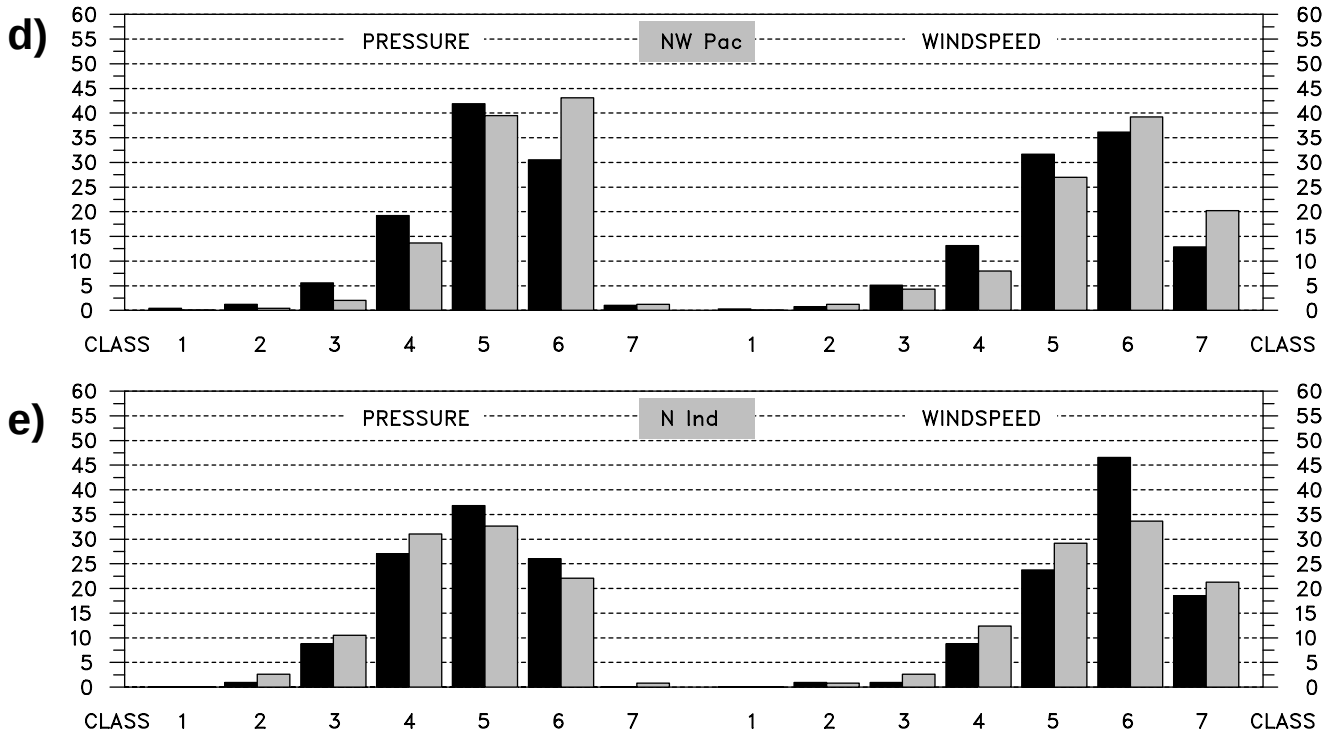

Fig. 12: **(continued)** Intensities of tropical storms for TSL_1 (black columns) and TSL_2 (grey columns) defined via the minimum pressure as well as via the maximum wind speed in 10 m distinguishing between the entire northwestern Pacific (d) and the northern Indian Ocean (e). The estimates have been obtained by dividing the numbers of storms in each class by the overall numbers of storms for the respective areas and the respective data sets. For the definition of the different classes see the text (section 4). Units are [%].

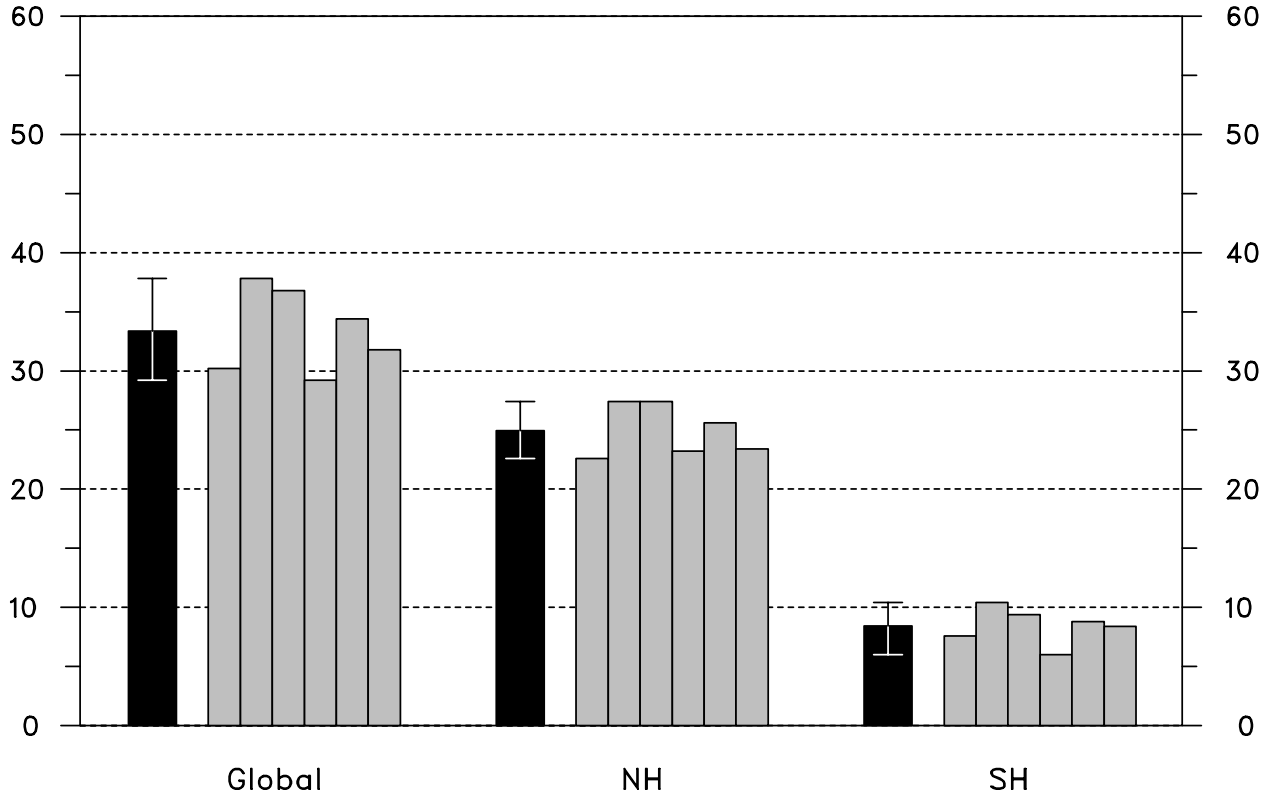

Fig. 13: As Fig. 6, but for TSL_2.

the months of February and August as representative months for the summer seasons in the Southern and in the Northern Hemisphere, respectively.

Figure 14 shows vertical cross-sections of the changes in the zonal mean temperatures defined as the difference between the long-term monthly mean values obtained from TSL_2 and TSL_1 for the two months. The cross-sections reveal a general warming in the troposphere and a cooling in the stratosphere. A maximum warming exceeding 5 °C in February (Fig. 14a) and 6 °C in August (Fig. 14b), respectively, occurs in the high tropical troposphere (centred at about 200 hPa), while in the lower troposphere the temperatures increase by 2 to 3 °C. As a consequence of the relatively strong warming at the high levels, the temperature stratification in the tropics is more stable in the future climate, so that the (upward) vertical motions are suppressed. According to the horizontal distributions of the temperature differences between 850 and 300 hPa (Fig. 15), the stabilization of the temperature stratification occurs virtually everywhere in the tropics. In addition to the Arctic (only in boreal winter) and the Antarctic regions we find a destabilization only over the continents during the local summer seasons, that is in Australia and southwestern Africa in February with not being significant, though, (Fig. 15a) and in the US as well as the Mediterranean area and the Near East in August (Fig. 15b).

As discussed in Gray (1979), a vertical wind shear influences the organized convection of a hurricane negatively, leading to a smaller number of TCs or less developed storms, respectively. During February the zonal component of the flow in the tropics is characterized by easterly winds in the lower and westerly winds in the upper troposphere (Fig. 16a), leading to a vertical wind shear in the tropics. In the Southern Hemisphere tropics, i.e., the zone between the equator and 40° S, the vertical wind shear is increased in the future due to an intensification of both the easterly winds in the lower and the westerly winds in the upper troposphere (Fig. 16b). As a consequence, the conditions for the development of TCs in the Southern Hemisphere are less favourable in the future. During August, on the other hand, the cross-section reveals easterly winds at all levels in the Northern Hemisphere tropics (Fig. 16c), so that there is hardly any vertical wind shear in this zone. But in the future climate the easterly winds are enhanced in the lower and reduced in the upper troposphere (Fig. 16d), indicating the tendency to create a vertical wind shear and, hence, less favourable conditions for the development of TCs in the Northern Hemisphere as well.

According to B95, the existence of large-scale convergence in the lower part of the trop-

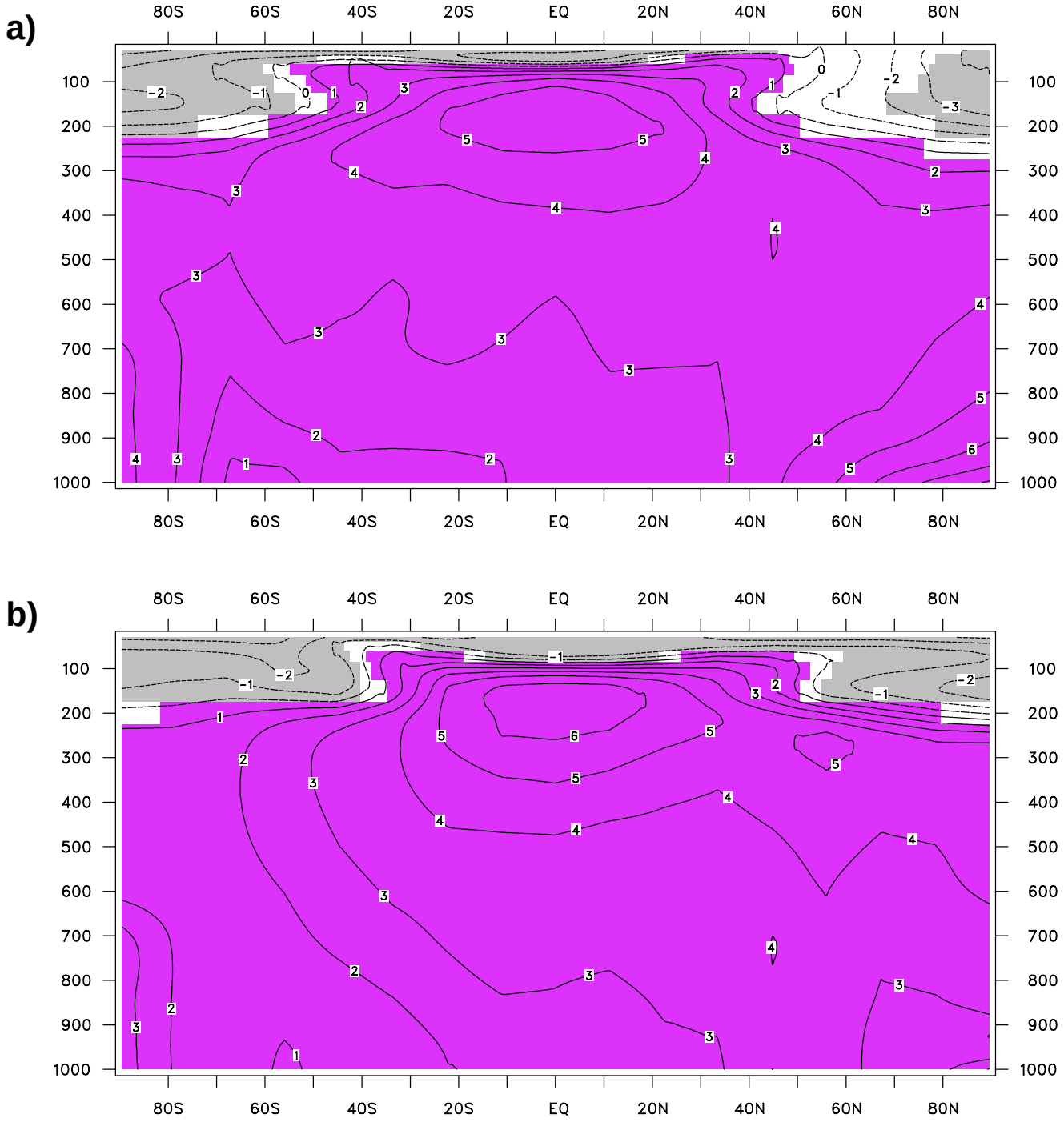

Fig. 14: Vertical cross-sections of the change in the monthly mean zonal mean temperatures between TSL_2 and TSL_1 (i.e., TSL_2 - TSL_1) for February (a) and August (b). Units are [°C], the contour interval is 1 °C. The significance at the 99%-level is marked by the shading.

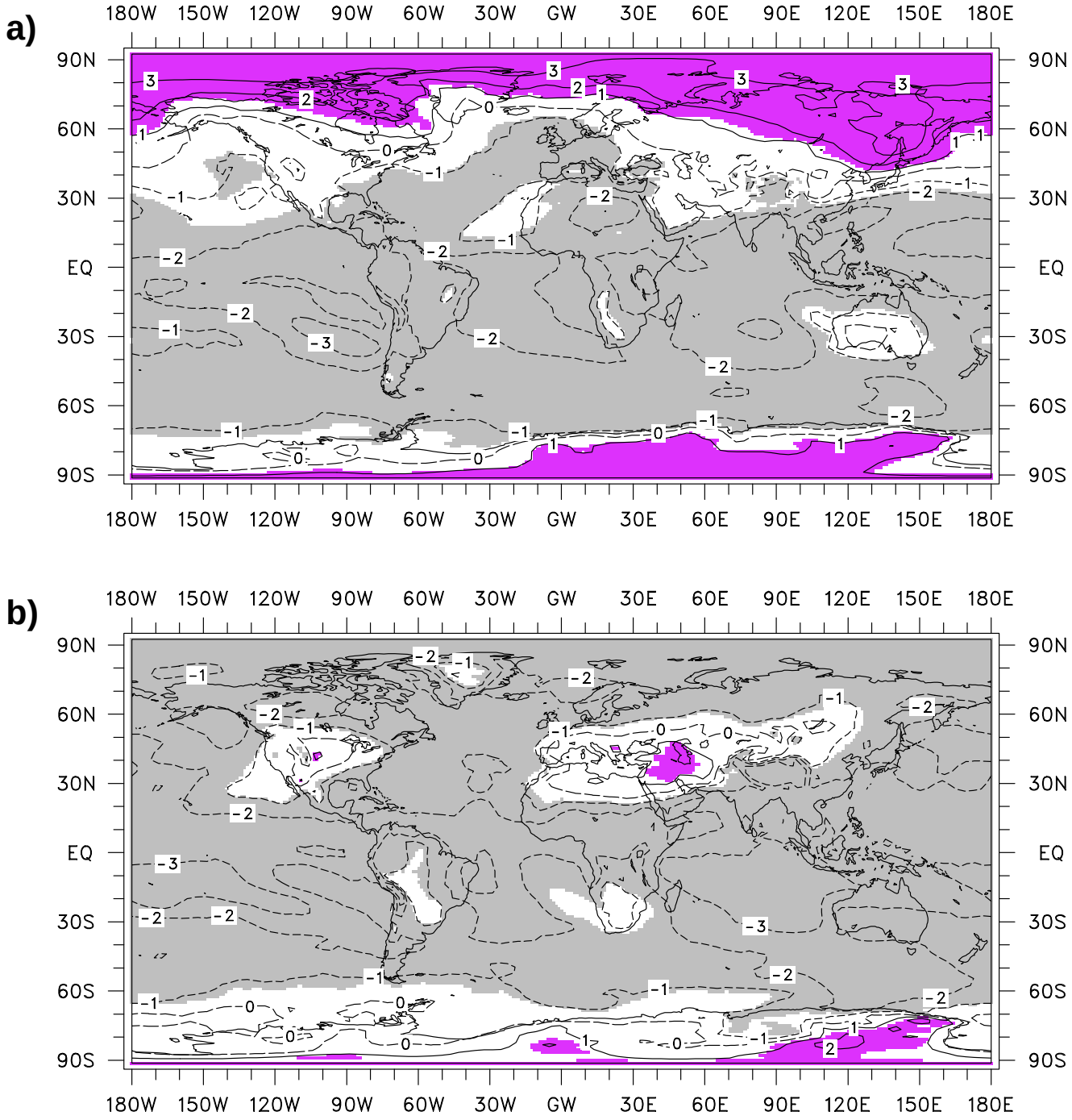

Fig. 15: Change in the monthly mean temperature difference between 850 and 300 hPa between TSL_2 and TSL_1 for February (a) and August (b). Units are [°C], the contour interval is 1 °C. The significance at the 99%-level is marked by the shading.

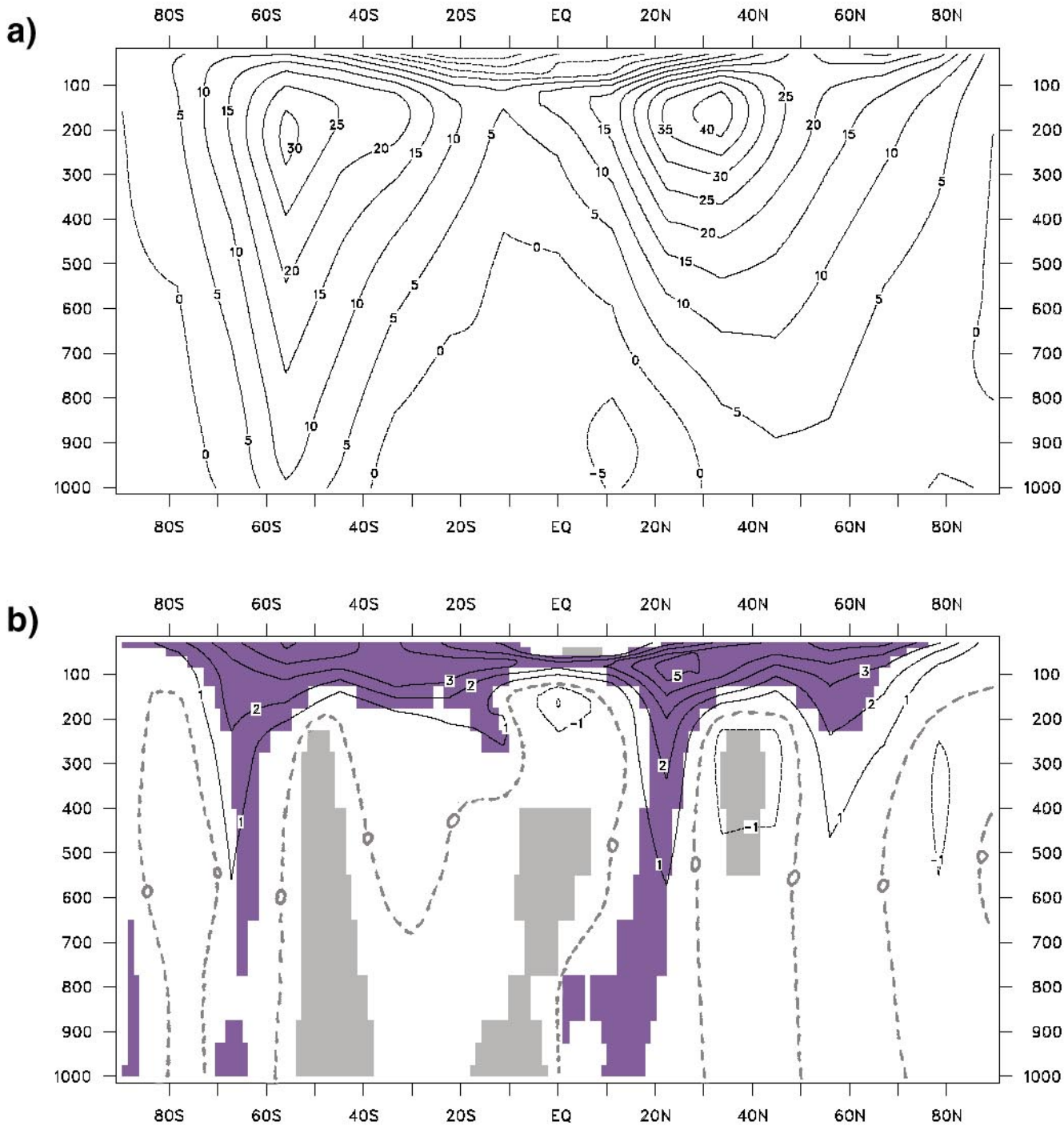

Fig. 16: Vertical cross-sections of the monthly mean zonal mean zonal wind component for TSL_1 (a) as well as of the change between TSL_2 and TSL_1 (b) for February. Units are [m/s], the contour interval is 5 m/s (a) and 1 m/s (b), respectively. The significance at the 99%-level is marked by the shading (b).

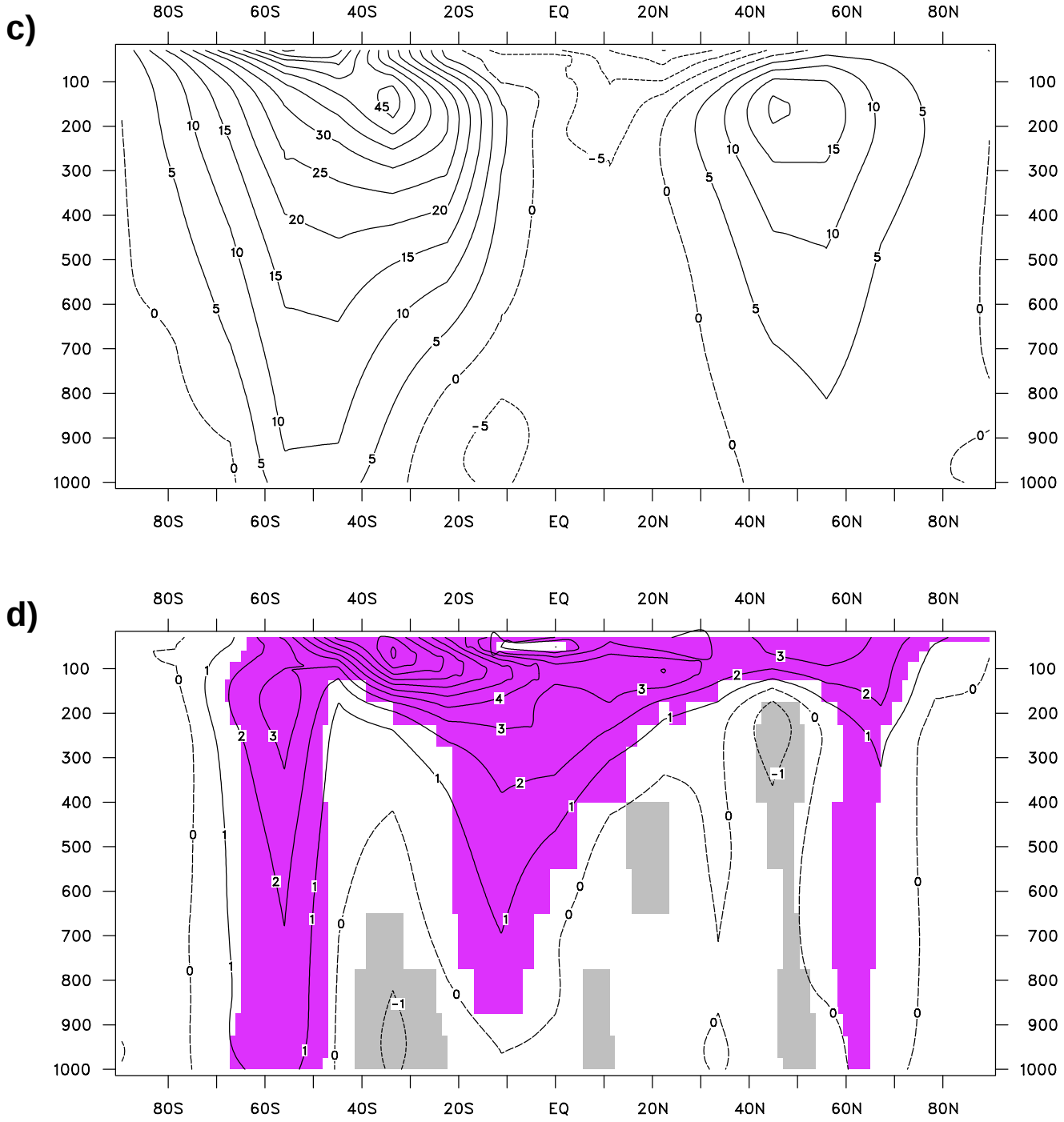

Fig. 16: **(continued)** Vertical cross-sections of the monthly mean zonal mean zonal wind component for TSL_1 (c) as well as of the change between TSL_2 and TSL_1 (d) for August. Units are [m/s], the contour interval is 5 m/s (c) and 1 m/s (d), respectively. The significance at the 99%-level is marked by the shading (b).

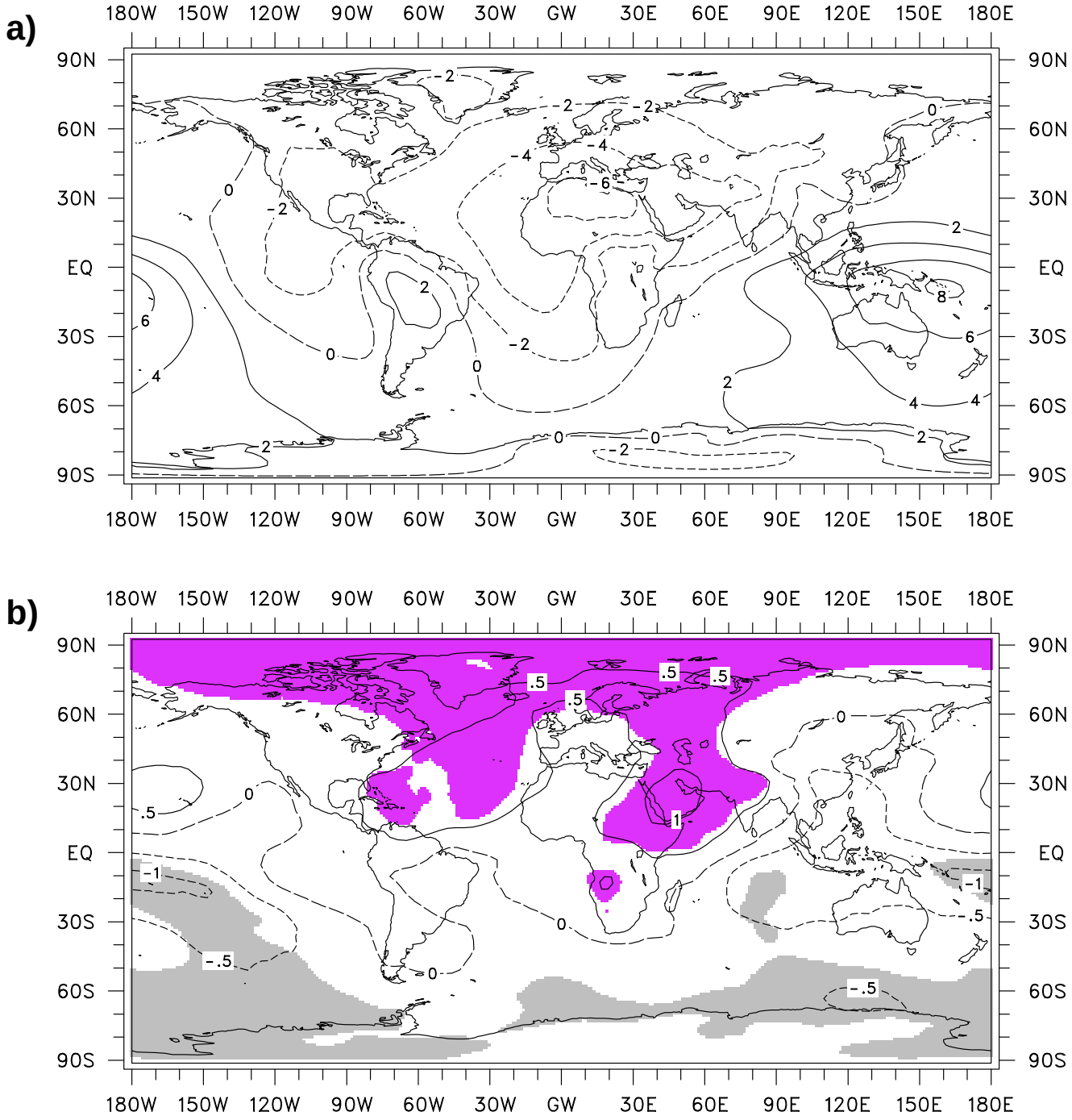

Fig. 17: Monthly mean velocity potential at 850 hPa for TSL_1 (a) as well as the change between TSL_2 and TSL_1 (b) for February. Units are [$(km)^2/s$], the contour interval is 2 $(km)^2/s$ (a) and 0.5 $(km)^2/s$ (b), respectively. The significance at the 99%-level is marked by the shading (b).

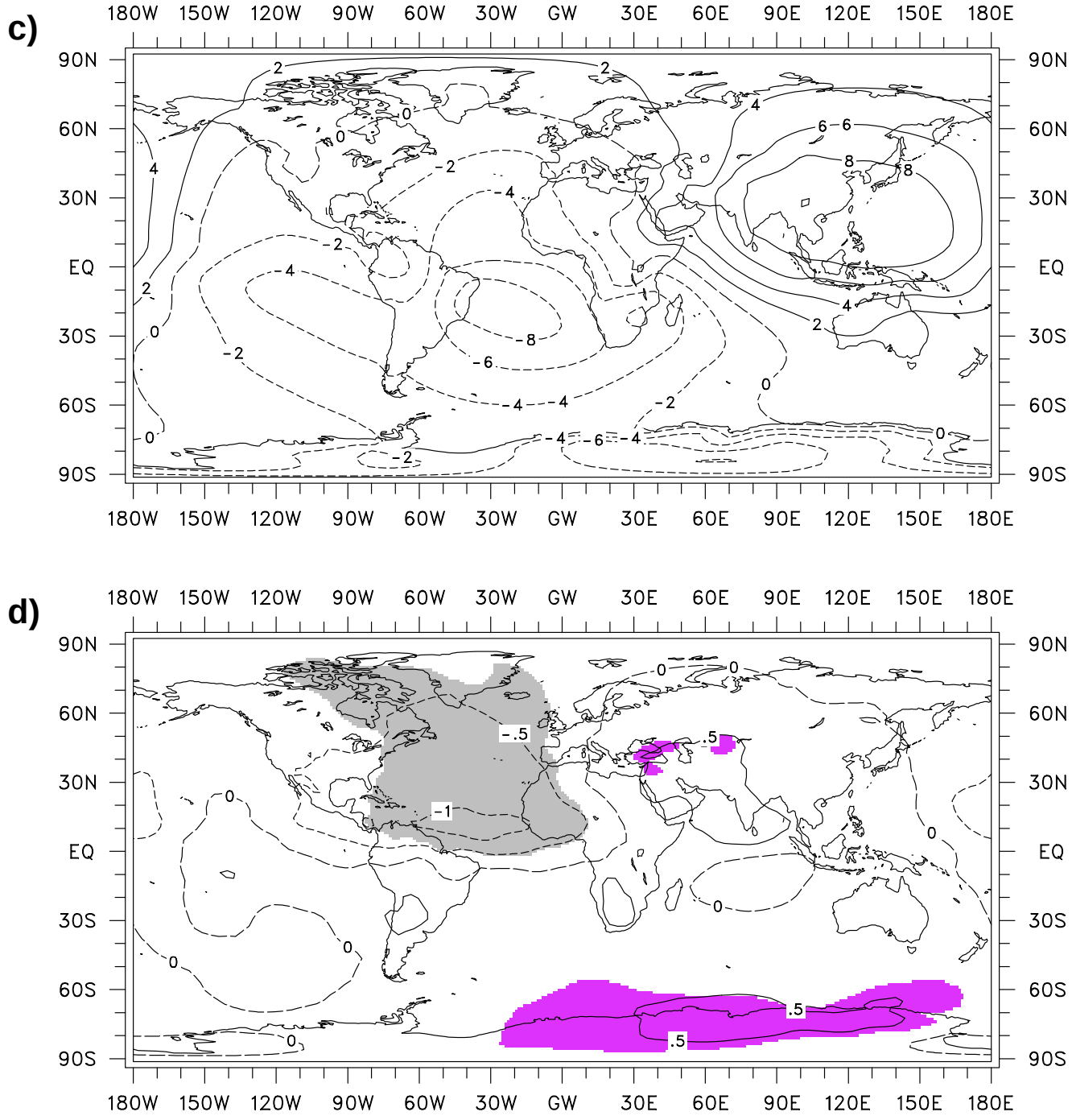

Fig. 17: **(continued)** Monthly mean velocity potential at 850 hPa for TSL_1 (c) as well as the change between TSL_2 and TSL_1 (d) for August. Units are $[(km)^2/s]$, the contour interval is 2 $(km)^2/s$ (c) and 0.5 $(km)^2/s$ (d), respectively. The significance at the 99%-level is marked by the shading (d).

osphere is a necessary condition for the development of TCs in those areas, where the Coriolis force is strong enough to provide the required convergence. During February such an area of convergence (expressed via the velocity potential) is located over the Indian and the Pacific Ocean, centred in the upward branch of the Walker Circulation near Indonesia (Fig. 17a). And consistent with the suggestion in B95, the model simulates a large number of TCs in these regions during austral summer (see Fig. 2d). In the future climate the convergence and, hence, the number of tropical storms is reduced in these regions (Fig. 17b). During August the area with the strongest large-scale convergence is shifted to the Northern Hemisphere and is centred over southeastern Asia (Fig. 17c). It is also in this area, where a large number of TCs can be found during boreal summer (see Fig. 2b). Also in the Caribbean and to the west of Mexico over the northeastern Pacific occur TCs frequently during this season, but as for the long-term mean values these regions are characterized by a relatively weak, though, large-scale divergence. This suggests that during certain periods large-scale convergence occurs in these regions. As for the future climate, we find a reduction of the convergence in the Caribbean and in the region west of Mexico, but no marked change over southeastern Asia (Fig. 17d).

Another change in the atmospheric circulation with a negative impact on the development on TCs is the reduction of the vorticity in the lower troposphere in those regions, where TCs typically occur. During February (here we show the Southern Hemisphere only) the simulations actually reveal such a change for the future, since over the Pacific and the Indian Ocean the relative vorticity at 850 hPa is considerably smaller in TSL_2 (Fig. 18b) than in TSL_1 (Fig. 18a). But during August (here we show the Northern Hemisphere only) we do not find a corresponding reduction of the relative vorticity over the western Pacific to the north of Indonesia or over the eastern Pacific to the west of Central America (Figs. 18c, d).

7. Concluding remarks

In this study we have investigated the ECHAM4 atmospheric GCM's ability to simulate tropical cyclones in the present-day climate and assessed the possible changes of the frequency and intensity of tropical storms in a warmer climate. This has been done on the basis of an extended time-slice experiment using ECHAM4 at a horizontal resolution of T106. The two time-slices cover a period of 30 years each representing both the present-day (1970-1999) and the future (warmer) climate (2060-2089).

The overall finding of our study is a substantial (about 25%) reduction of the number of

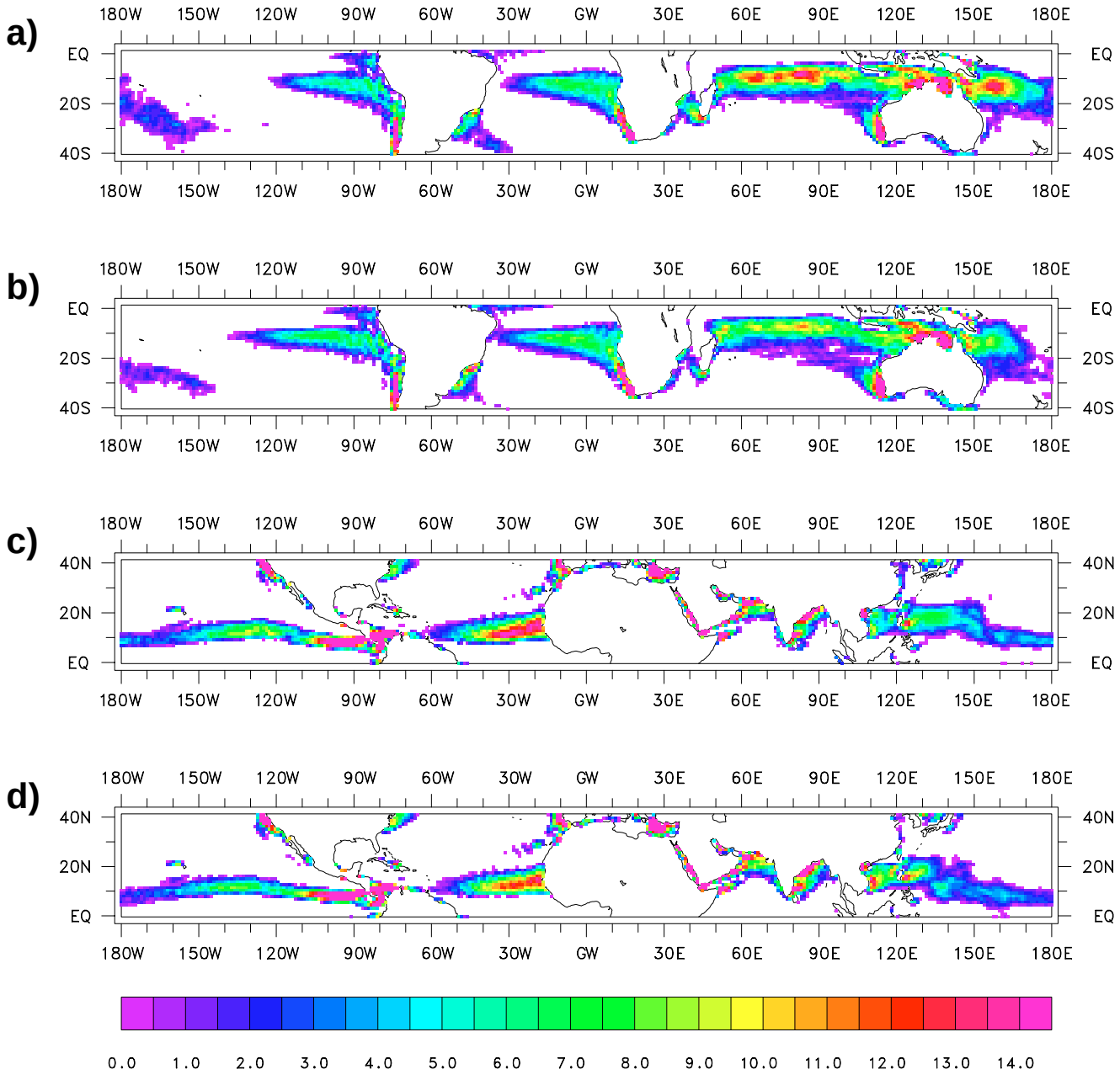

Fig. 18: Monthly mean relative vorticity at 850 hPa for TSL_1 and TSL_2 for February in the Southern Hemisphere tropics (a, b) and for August in the Northern Hemisphere tropics (c, d). Units are [10^{-5}/s], only positive values are shown.

tropical storms in the future climate. The reduction is somewhat larger in the Southern than in the Northern Hemisphere. Along with this reduction of the frequency goes a general reduction of the intensity of TCs. The decrease of the number of TCs seems to be due to large-scale changes of the circulation in the tropics leading to less favourable dynamical conditions for the developments of storms, while one would expect more and/or more intense cyclones due to the general warming of the SSTs in the tropics. As for the reduction of the frequency in the future, our finding is in general agreement with the main result by B96, who used the ECHAM3 model in a study similar to ours, but in disagreement with the findings by Broccoli and Manabe (1990) or Haarsma et al. (1993), whose studies were based on low-resolution coupled GCMs. Broccoli and Manabe (1990) obtained, however, a quite different result, i.e., a reduction of the number of TCs, when the clouds were predicted by the model. In a study using a high-resolution hurricane prediction model Knutson et al. (1998) and Knutson and Tuleya (1999) found, on the other hand, an intensification of TCs over the northwestern Pacific in a warmer climate.

As pointed out by the authors, the robustness of the results obtained in B96 was questionable due to the comparatively short integration time of 5 years for their time-slices. By using time-slices of 30 years we have been able to considerably reduce this source of uncertainty and also to reassure the finding by B96, since ours is in general agreement with theirs. Different to B95 and B96, who were able to identify rather realistic TCs in their simulations with ECHAM3, the tropical storms simulated by ECHAM4 are by far too weak and, hence, occur much less frequently than in reality, i.e., at about 55% of the time. The ECHAM4 model has undergone a number of major changes in both the numerical methods and the physical parameterizations compared to ECHAM3 (Roeckner et al., 1996a), which apparently have affected the simulation of TCs in a very negative way, and it would be the subject of an extensive study of its own to find out, which changes may have caused the degeneration of the model with regard to the simulation of tropical storms. But this discrepancy between the two versions of the ECHAM model clearly shows, how crucially the simulation of TCs depends on the physical parameterizations of the GCM.

In the light of this behaviour of the ECHAM model we are not as affirmative as B96 in answering the question, whether GCMs are the appropriate tools in explaining the mechanisms between greenhouse warming and tropical storm activity, which was raised by Broccoli and Manabe (1990). Firstly, there seems to be a very fine balance between the different model components, at which GCMs are able to simulate tropical storms reasonably well. And secondly,

the changes in the development of TCs seem to be very much determined by the changes in the large-scale circulation in the tropics, which depending on the respective GCM may lead to more or less favourable conditions for the development of tropical storms in the future.

Acknowledgements

I would like to thank Henrik Feddersen for his comments on an earlier version of this report. This work was supported by the “Environment and Climate Programme” under contract ENV4-CT97-0640, “An enhanced resolution modelling study on anthropogenic climate change”.

References

Annamalai, H., Slingo, J. M., Sperber, K. R. and Hodges, K. 1999. The mean evolution and variability of the Asian summer monsoon: Comparison of ECMWF and NCEP-NCAR reanalyses. *Mon. Wea. Rev.* **127**, 1157-186.

Bacher, A., Oberhuber, J. M. and Roeckner, E. 1998. ENSO dynamics and seasonal cycle in the tropical Pacific as simulated by the ECHAM4/OPYC3 coupled general circulation model. *Clim. Dyn.* **14**, 431-450.

Bengtsson, L., Botzet, M. and Esch, M. 1995. Hurricane-type vortices in a general circulation model. *Tellus* **47A**, 175-196.

Bengtsson, L., Botzet, M. and Esch, M. 1996. Will greenhouse gas-induced warming over the next 50 years lead to higher frequency and greater intensity of hurricanes? *Tellus* **48A**, 57-73.

Broccoli, A. J. and Manabe, S. 1990. Can existing climate models be used to study anthropogenic changes in tropical cyclone climate? *Geophys. Res. Lett.* **17**, 1917-1920.

Chan, J. C. L. 1985. Tropical cyclone activity in the northwest Pacific in relation to the El Niño/Southern Oscillation phenomenon. *Mon. Wea. Rev.* **113**, 599-606.

Chan, J. C. L. and Shi, J. 1996. Long-term trends and interannual variability in tropical cyclone activity over the western North Pacific. *Geophys. Res. Lett.* **23**, 2765-2767.

Cubasch, U., Hasselmann, K., Höck, H., Maier-Reimer, E., Mikolajewitz, U., Santer, B. D. and Sausen, R. 1992. Time-dependent greenhouse warming computations with a coupled ocean-atmosphere model. *Clim. Dyn.* **8**, 55-69.

Evans, J.L. and Allan, R. J. 1992. El Niño/Southern Oscillation modification of monsoon and tropical cyclone activity in the Australian region. *Int. J. Climatol.* **12**, 611-623.

Gray, W. 1979. Hurricanes: their formation, structure and likely role in the tropical circulation. *Meteorology over the Tropical Oceans*, D. B. Shaw (ed.), *Roy. Meteorol. Soc.*, 155-218.

Haarsma, R. J., Mitchell, J. F. B. and Senior, C. A. 1993. Tropical disturbances in a GCM. *Clim. Dyn.* **8**, 247-257.

Henderson-Sellers, A., Zhang, H., Berz, G., Emanuel, K., Gray, W., Landsea, C., Holland, G., Lighthill, J., Shieh, S.-L., Webster, P. and McGuffie, K. 1998. Tropical cyclones and global climate change: A post-IPCC assessment. *Bull. Amer. Met. Soc.* **79**, 19-39.

Holland, G. J. 1997. The maximum potential intensity of tropical cyclones. *J. Atmos. Sci.* **54**, 2519-2541.

Houghton, J. T., Callandar, B. A. and Varney, S. K. (eds.) 1992. *Climate Change 1992: The supplementary report to the IPCC scientific assessment.* Cambridge University Press, 198 pp.

Houghton, J. T., Jenkins, G. J. and Ephraums J. J. (eds.) 1990. *Climate Change. The IPCC scientific assessment.* Cambridge University Press, 364 pp.

Houghton, J. T., Meira Filho, L. G., Callandar, B. A., Harris, N., Kattenberg, A. and Maskell, K. (eds.) 1996. *Climate Change 1995. The science of climate change.* Cambridge University Press, 572 pp.

Jones, C. G. and Thorncroft, C. D. 1998. The role of El Niño in the Atlantic tropical cyclone activity. *Weather* **53**, 324-336.

Knutson, T. R. and Tuleya, R. E. 1999. Increased hurricane intensities with CO_2-induced warming as simulated using the GFDL hurricane prediction system. *Clim. Dyn.* **15**, 503-519.

Knutson, T. R., Tuleya, R. E. and Kurihara, Y. 1998. Simulated increase of hurricane intensities in a CO_2-warmed climate. *Science* **279**, 1018-1020.

Kunkel, K. E., Pielke, R. A. Jr. and Changnon, S. A. 1999. Temporal fluctuations in weather and climate extremes that cause economic and human health impacts: A review. *Bull. Amer. Met. Soc.* **80**, 1077-1098.

Kurihara, Y., Tuleya, R. E. and Bender, M. A. 1998. The GFDL hurricane prediction system and its performance in the 1995 hurricane season. *Mon. Wea. Rev.* **126**, 1306-1322.

Lander, M. A. 1994. An exploratory analysis of the relationship between tropical storm formation in the western North Pacific and ENSO. *Mon. Wea. Rev.* **122**, 636-651.

Landsea, C. W., Nicholls, N., Gray, W. M. and Avila, L. A. 1996. Downward trends in the frequency of intense Atlantic hurricanes during the past five decades. *Geophys. Res. Lett.* **23**, 1697-1700.

Manabe, S., Stouffer, R. J., Spelman, M. J. and Bryan, K. 1991. Transient responses of a coupled ocean-atmosphere model to gradual changes of atmospheric CO_2. Part I: annual mean response. *J. Climate* **4**, 785-818.

May, W. 1999. A time-slice experiment with the ECHAM4 A-GCM at high resolution: The experimental design and the assessment of climate change as compared to a greenhouse gas experiment with ECHAM4/OPYC at low resolution. *DMI Scientific Report* **99-2**, 93 pp.

May, W. and Roeckner, E. 2000. A time-slice experiment with the ECHAM4 AGCM at high resolution: The impact of horizontal resolution on annual mean climate change. *Clim. Dyn.*, in press.

Mitchell, J. F. B., Davis, R. A., Ingram, W. J. and Senior, C. A. 1995. On surface temperature, greenhouse gases and aerosols: models and observations. *J. Climate* **8**, 2364-2386.

Mitchell, J. F. B., Johns, T. C. 1997. On modification of global warming by sulfate aerosols. *J. Climate* **10**, 245-267.

Neumann, C. J. 1993. Global overview. Global guide to tropical cyclone forecasting. *WMO/TC* **560**.

Nicholls, N. 1984. The Southern Oscillation, sea surface temperature and interannual fluctuations in Australian tropical cyclone activity. *J. Climatol.* **4**, 661-670.

Nicholls, N., Landsea, C. and Gill, J. 1998. Recent trends in Australian region tropical cyclone activity. *Meteorol. Atmos. Phys.* **65**, 195-205.

Oberhuber, J. M. 1993. Simulation of the Atlantic circulation with a couple sea-ice - mixed layer - isopycnal general circulation model. Part I: Model description. *J. Phys. Oceanogr.* **22**, 808-829.

Revell, C. G., and Goulter, S. W. 1986. South Pacific tropical cyclones and the Southern Oscillation. *Mon. Wea. Rev.* **114**, 138-1145.

Roeckner, E., Arpe, K., Bengtsson, L., Christoph, M., Claussen, M., Dümenil, L., Esch, M., Giorgetta, M., Schlese, U. and Schulzweida, U. 1996a. The atmospheric general circulation model ECHAM-4: Model description and simulation of present-day climate. *MPI-Report* **218**, 90 pp.

Roeckner, E., Bengtsson, L., Feichter, J., Lelieveld, J. and Rodhe, H. 1999. Transient climate change simulations wit a coupled atmosphere-ocean GCM including the tropospheric sulfur cycle. *J. Climate* **12**, 3004-3932.

Roeckner, E., Oberhuber, M., Bacher, A., Christoph, M., Kirchner, I. 1996b. ENSO variability and atmospheric response an a coupled atmosphere-ocean GCM. *Clim. Dyn.* **12**, 737-754.

Serrano, E. 1997. Tropical cyclones. *ECMWF Re-analysis Project Report Series* **5**, 29 pp.

Shen, W., Tuleya, R. E., and Ginis, I. 2000. A sensitivity study of the thermodynamic environment on GFDL model hurricane intensity: Implications for global warming. *J. Climate* **13**, 109-121.

Stendel, M. and Roeckner, E. 1998. Impacts of horizontal resolution on simulated climate statistics in ECHAM4. *MPI-Report* **253**, 57 pp.

Walsh, K. 1997. Objective detection of tropical cyclones in high-resolution analysis. *Mon. Wea. Rev.*, **125**, 1767-1779.

Walsh, K. and Watterson, I. G. 1997. Tropical cyclone-like vortices in a limited area model: Comparison with observed climatology. *J. Climate* **10**, 2240-2259.

Watson, R. T., Zinyowewa, M. C. and Moss, R. H. (eds.) 1996. *Climate Change 1995. Impacts, adaptations and mitigation of climate change.* Cambridge University Press, 879 pp.

Table 1:

Area	Ratio (%)
Globe	54.7
N Hemisphere	58.5
S Hemisphere	46.4
NW Atlantic	20.5
NE Pacific	36.6
NW Pacific	83.8
N Indian	47.9
S Indian	48.8
Australia	49.8
S Pacific	35.6

Ratio between the numbers of tropical storms obtained from TSL_1 (1970-1999) and from observations (1958-1977; Gray (1979)) distinguishing between different regions (Bengtsson et al., 1995).

Table 2:

Month	N Hemisphere Ratio (%)	S Hemisphere Ratio (%)
January	104.8	40.4
February	188.9	46.9
March	244.4	41.1
April	140.0	34.9
May	132.2	86.7
June	85.2	n.a.
July	58.5	n.a.
August	33.3	n.a.
September	38.3	n.a.
October	51.9	25.0
November	62.0	46.7
December	86.7	44.4

Ratio between the numbers of tropical storms obtained from TSL_1 (1970-1999) and from observations (1958-1977; Gray (1979)) for different months distinguishing between the Northern and the Southern Hemisphere. The term “n.a.” has been used for those months, where according to the observations no tropical storms occur in the Southern Hemisphere.

Table 3:

Area	Rel. Range (%)	
	TSL_1	TSL_2
Globe	22.2	25.8
N Hemisphere	28.8	19.3
S Hemisphere	26.4	52.2
NW Atlantic	188.9	112.5
NE Pacific	93.9	90.3
NW Pacific	30.0	34.4
N Indian	39.1	63.7
S Indian	58.5	136.7
Australia	50.6	69.1
S Pacific	85.7	145.5

Relative range of the numbers of tropical storms obtained from TSL_1 (1970-1999) and TSL_2 (2060-2089) for 6 consecutive 5-year periods distinguishing between different regions. The estimates are defined as the differences between the maximum and the minimum number of tropical storms occurring in an individual 5-year period divided by the long-term mean values for the respective regions.

Table 4:

Area	Ratio (%)	Ratio (%) B96
Globe	77.1	68.2
N Hemisphere	78.1	74.7
S Hemisphere	74.2	43.3
NW Atlantic	59.3	87.0
NE Pacific	76.9	79.5
NW Pacific	74.0	65.9
N Indian	122.8	90.0
S Indian	64.2	35.9
Australia	90.3	46.8
S Pacific	52.4	55.0
Others	60.0	42.9

Ratio between the numbers of tropical storms for TSL_2 (2060-2089) and TSL_1 (1970-1999) as well as the relative change in the number of tropical storms according to Bengtsson et al. (1996) distinguishing between different regions.

Table 5:

Month	N Hem Ratio (%)	S Hem Ratio (%)	NW Pac Ratio (%)	N Ind Ratio (%)
January	63.6	93.2	42.1	200.0
February	76.5	66.3	92.3	33.3
March	59.1	62.1	59.1	n.a.
April	61.9	40.9	70.0	0.0
May	56.5	38.5	55.1	68.8
June	55.6	44.4	53.9	116.7
July	78.1	125.0	68.5	62.8
August	82.6	33.3	74.6	300.0
September	87.9	233.3	86.7	237.5
October	86.2	0.0	90.6	87.5
November	95.0	71.4	89.3	113.6
December	156.7	97.9	116.7	316.7

Ratio between the numbers of tropical storms for TSL_2 and TSL_1 for different months distinguishing between the Northern and the Southern Hemisphere, the northwestern Pacific and the northern Indian Ocean, respectively. The term “n.a.” has been used for those months, where according to TSL_1 no tropical storms occur over the northern Indian Ocean.

The Danish Climate Centre

The Danish Climate Centre was established at the Danish Meteorological Institute in 1998. The main objective is to project climate into the 21 st century for studies of impacts of climate change on various sectors and ecosystems in Denmark, Greenland and the Faroes.

The Climate Centre activities include development of new and improved methods for satellite based climate monitoring, studies of climate processes (including sun-climate relations, greenhouse effect, the role of ozone, and air/sea/sea-ice interactions), development of global and regional climate models, seasonal prediction, and preparation of global and regional climate scenarios for impact studies.

The Danish Climate Centre is organised with a secretariat in the Research and Development Department, and it is co-ordinated by the Director of the Department. It has activities also in the Weather Service Department and the Observation Department, and it is supported by the Data Processing Department.

The Danish Climate Centre has established the Danish Climate Forum for researchers in climate and climate related issues and for others having an interest in the Danish Climate Centre activities. The Centre issues a quarterly newsletter KlimaNyt (in Danish).

DMI has been doing climate monitoring and research since its foundation in 1872, and establishment of the Danish Climate Centre has strengthened both the climate research at DMI and the national and international research collaboration.

Previous reports from the Danish Climate Centre:

- Dansk Klimaforum 29.-30. april 1998. (Opening of Danish Climate Centre and abstracts and reports from Danish Climate Forum workshop). *Climate Centre Report 98-1* (in Danish).
- Danish Climate Day 1999. *Climate Centre Report 99-1*.
- Dansk Klimaforum 12. april 1999. Workshop: Klimatisk variabilitet i Nordatlanten på tidsskalaer fra årtier til århundreder. *Climate Centre Report 99-2* (in Danish).
- Luftfart og den globale atmosfære, Danmarks Meteorologiske Instituts oversættelse af IPPC's særrapport "Aviation and the Global Atmosphere, Summary for Policymakers". *Climate Centre Report 99-3* (in Danish).
- Forskning og Samarbejde 1998-1999, *Climate Centre Report 00-1* (in Danish).
- Drivhuseffekten og regionale klimaændringer, *Climate Centre Report 00-2* (in Danish).
- Emissionsscenarier, Danmarks Meteorologiske Instituts oversættelse af IPPC's særrapport "Emissions Scenarios, Summary for Policymakers". *Climate Centre Report 00-3* (in Danish).
- Metoder mødes: Geofysik og emner af samfundsmæssig interesse. Dansk Klimaforums Workshop 15.-16. maj 2000. *Climate Centre Report 00-4* (in Danish).